Crystal Structure of $Ba_{12}Co_{11}O_{33}$. Reinvestigation Using the Superspace Group Approach of Orthorhombic Oxides $A_{1+x}(A'_xB_{1-x})O_3$ Based on $[A_8O_{24}]$ and $[A_8A'_2O_{18}]$ Layers

J. Darriet,*,† L. Elcoro,‡ A. El Abed,†,§ E. Gaudin,† and J. M. Perez-Mato‡

Institut de Chimie de la Matière Condensée de Bordeaux (ICMCB-CNRS), 87, Avenue du Dr. A. Schweitzer, 33608, Pessac Cedex, France, Departamento de Fisica de la Materia Condensada, Facultad de Ciencias, Universidad del Pais Vasco, Apdo 644, 48080 Bilbao, Spain, and Laboratoire de Physique des Solides, Faculté des Sciences, Université Mohamed 1er, Oujda, Morocco

Received March 11, 2002. Revised Manuscript Received May 7, 2002

We report the structure determination on a single crystal of $Ba_{12}Co_{11}O_{33}$, which belongs to the family of 1-dimensional structures related to the 2H hexagonal perovskite. The structure can be derived from the hcp stacking of $[Ba_8Co_2O_{18}]$ and $[Ba_8O_{24}]$ layers. Assuming a similitude in the building principle with that present in the homologue rhombohedral series based on $[A_3A'O_6]$ and $[A_3O_9]$ layers, a generic model within the superspace formalism of the whole family is proposed and used successfully for $Ba_{12}Co_{11}O_{33}$. Two different strategies are presented. The first one considers the structure as a commensurate modulated composite containing two subsystems $[CoO_3]$ and [Ba]. With the $[CoO_3]$ subsystem chosen as the reference, the superspace group is $Fddd(00\gamma_C)0s0$ with $a = 11.4129(2)$ Å, $b = 19.7677(2)$ Å, $c_1 = 2.4722(1)$ Å, and $q = (6/11)c_1^*$ ($Z = 8$ for the formula $Ba_{12/11}CoO_3$). The final global R value is 4.46% for 4625 independent reflections (at a $I/\sigma(I) > 3$ level) and only 123 refineable parameters. The second model follows the natural description of the structure as formed by the uniform hcp stacking of the two types of layers $[Ba_8Co_2O_{18}]$ and $[Ba_8O_{24}]$. The structure is formulated as $BaCo_{11/12}O_{33/12}$ ($Z = 16$) and considered to be a commensurate modulated phase with crenel occupational modulations. The superspace group can be denoted as $Xdcd(00\gamma_L)qq0$ with $a = 11.4129(2)$ Å, $b = 19.7677(2)$ Å, $c = 4.5324(1)$ Å, and $q = (1/6)c^*$. The final global R value is 4.36% for the same number of independent reflections and 151 refineable parameters. Both approaches yield similar results, demonstrating for the first time the feasibility of refining these structures as layerlike modulated structures, instead of composites. The chains consist of polyhedra sharing faces formed by 10 consecutive CoO_6 octahedra followed by one trigonal prism. Previous models based on simulated and high-resolution electron microscopy images are refuted.

1. Introduction

Polytypism and intergrowth polytypoids are well-known in solid-state chemistry. They define a series of structures which can be regarded as being built up by the stacking of layers with very close structure but different stacking sequences. Typical examples of polytypism are the hexagonal perovskites based on the parent 2H-ABO_3. This parent structure is formed by chains of BO_6 octahedra sharing faces parallel to the c axis as a consequence of the hexagonal stacking of the AO_3 layers where the B cations occupy the octahedral sites.[1] In comparison, the cubic perovskite corresponds to the cubic stacking of the same type of AO_3 layers. In this case, the BO_6 octahedra share corners forming a 3-dimensional network. Between these two limits, many polytypes have been observed resulting from different sequences that mix these two types of stacking. The basic principle of these polytypes was first described a long time ago.[2]

When a homologous series exists where the layer sequence varies among the compounds keeping a one-to-one relationship between composition and sequence, we can talk of *polytypoids*. In most cases, for complex compositions their structure can be regarded as the *intergrowth* of "blocks" of different (simpler) compositions of the same series.

Recently, a model was proposed to explain anionic and cationic deficient hexagonal perovskites related to the 2H-polytypes.[3] In particular, a series of trigonal and rhombohedral compounds have been described as a single family of polytypoids constituted by trigonal layers of types A_3O_9 ($3 \times AO_3$) and $A_3A'O_6$, the latter resulting from the former by substitution of three oxygen atoms by one A′ atom (see Figure 1a,b). The

* To whom correspondence should be addressed. ICMCB-CNRS, 87, Avenue du Dr. A. Schweitzer, 33608 Pessac Cedex, France. Tel.: 33 (0)5 56 84 62 59. Fax: 33(0)5 56 84 27 61. E-mail: darriet@icmcb.u-bordeaux.fr.

† ICMCB-CNRS.

‡ Universidad del Pais Vasco.

§ Université Mohamed 1er.

(1) Lander, J. *Acta Crystallogr.* **1951**, *4*, 148.

(2) Katz, L.; Ward, R. *Inorg. Chem.* **1963**, *3* (2), 205.

(3) Darriet, J.; Subramanian, M. A. *J. Mater. Chem.* **1995**, *5* (4), 543.

10.1021/cm0211610 CCC: $22.00
Published on Web 07/23/2002

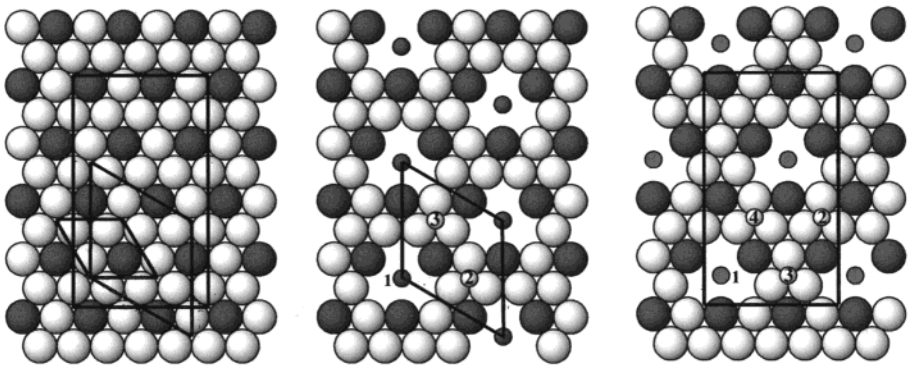

Figure 1. Schematic representations of A_8O_{24} (a), $A_3A'O_6$ (b), and $A_8A'_2O_{18}$ (c) layers. The metric relationships of the unit cells in the *xy* plane is outlined in (a). The origins corresponding to equivalent but distinct (translated) layers which can be present in the layer stacking sequences are shown for the A′ substituted layers (b) and (c).

hexagonal stacking of these layers creates, besides octahedral sites occupied by the B cations, some prismatic sites (A′ site) with triangular bases, which leads to a new family of phases with the general formula $A_{3n+3m}A'_nB_{3m+n}O_{9m+6n}$, where m/n is the relative proportion of $[A_3O_9]$ and $[A_3A'O_6]$ layers. These structures can then be seen as a set of $[A'B]O_3$ chains parallel to the *c* axis separated by the A atoms and formed by trigonal prisms ($A'O_6$) and octahedra (BO_6) sharing faces. In an idealized configuration of perfect rigid layers, the trigonal prisms would have double the *z* height (c_{2H}) than the octahedra ($0.5c_{2H}$). The general formula of the whole family can be expressed in an equivalent way as $A_{1+x}(A'_xB_{1-x})O_3$ with $x = n/(3m + 2n)$ so that the composition variable x can be envisaged to be any number between the two limits 0 and 1/2. A value of $x = 0$ corresponds to the reference 2H hexagonal perovskite (only face sharing octahedra), while $x = 1/2$ is represented by the Sr_4PtO_6[4] prototype where all the layers have the $A_3A'O_6$ composition and the sequence along the chains is one octahedron plus one trigonal prism. In general, if $x = p/q$ (where p and q are integers), p represents the number of trigonal prisms and $(q - p)$ represents the number of octahedra in the sequence along the columns. For instance, $A_6A'B_4O_{15}$ corresponds to $n = 1$ and $m = 1$ and $x = 1/5$. The chains are then formed by four octahedra separated by one $A'O_6$ trigonal prism (see Figure 2). From the proposed basic principle,[3] it is possible to imagine a series of structures that contain, depending on the composition, different sequences of octahedra and trigonal prisms within the chains. These predictions have been confirmed experimentally by the discovery of about 40 new phases belonging to this family.[5−22] It can also be shown that $BaNi_{0.83}O_{2.5}$[23] and the low-temperature form of $SrCoO_{2.5}$[24−27] belong to this series and must be correctly formulated as $A_6B_5O_{15}$[3,28] (A = Sr, Ba; B = Co, Ni).

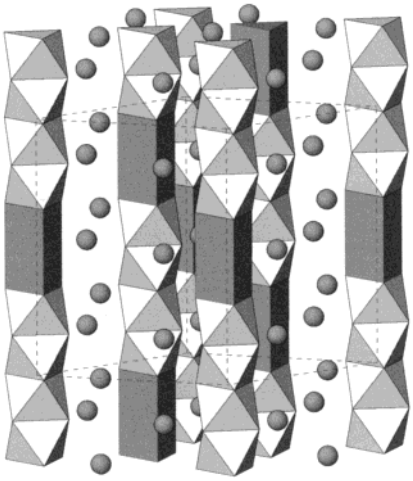

Figure 2. Schematic representation of the rhombohedral $A_6A'B_5O_{15}$-type structure.

(4) Randall, J. J.; Katz, L. *Acta Cystallogr.* **1959**, *12*, 519.
(5) Perez-Mato, J. M.; Zakhour-Nakhl, M.; Weill, F.; Darriet, J. *J. Mater. Chem.* **1999**, *9*, 2795−2808.
(6) Dussarrat, C.; Fompeyrine, J.; Darriet, J. *Eur. J. Solid State Inorg. Chem.* **1995**, *32*, 3.
(7) Abraham, F.; Minaud, S.; Renard, C. *J. Mater. Chem.* **1994**, *4*, 1763.
(8) Huvé, M.; Renard, C.; Abraham, F.; Van Tendeloo, G.; Amelinckx, S. *J. Solid State Chem.* **1998**, *135*, 1.
(9) Ukei, K.; Yamamoto, A.; Watanabe, Y.; Shishido, T.; Fukuda, T. *Acta Crystallogr.* **1993**, *B49*, 67.
(10) Battle, P. D.; Blake, G. R.; Sloan, J.; Vente, J. F. *J. Solid State Chem.* **1998**, *136*, 103.
(11) Blake, G. R.; Sloan, J.; Vente, J. F.; Battle, P. D. *Chem. Mater.* **1998**, *10*, 3536.
(12) Cussen, E. J.; Vente, J. F.; Battle, P. D. *J. Am. Chem. Soc.* **1999**, *121*, 3958.
(13) Zakhour-Nakhl, M.; Claridge, J. B.; Darriet, J.; Weill, F.; zur Loye, H.-C.; Perez-Mato, J. M. *J. Am. Chem. Soc.* **2000**, *122*, 1618−1623.
(14) Evain, M.; Boucher, F.; Gourdon, O.; Petricek, V.; Dusek, M.; Bedzdicka, P. *Chem. Mater.* **1998**, *10*, 3068−3076.
(15) Gourdon, O.; Petricek, V.; Dusek; M.; Bezdicka, P.; Durovic, S.; Gyepesova, D.; Evain, M. *Acta Crystallogr.* **1999**, *B55*, 841.
(16) Boulahya, K.; Parras, M.; Gonzalez-Calbet, J. M. *Chem. Mater.* **2000**, *12*, 25−32.
(17) Boulahya, K.; Parras, M.; Gonzalez-Calbet, J. M. *J. Solid State Chem.* **1999**, *142*, 419−427.
(18) Boulahya, K.; Parras, M.; Gonzalez-Calbet, J. M. *J. Solid State Chem.* **1999**, *145*, 116−127.
(19) Zakhour-Nakhl, M.; Darriet J.; Claridge, J. B.; zur Loye, H.-C.; Perez-Mato, J. M. *Int J. Inorg. Mater.* **2000**, *2*, 503.
(20) Zakhour-Nakhl, M.; Weill, F.; Darriet J.; Perez-Mato, J. M. *Int J. Inorg. Mater.* **2000**, *2*, 71.
(21) Stitzer, K. E.; Smith, M. D.; Darriet, J.; zur Loye, H.-C. *Chem. Commun.* **2001**, 1680.
(22) Stitzer, El Abed, A.; Darriet, J.; zur Loye, H.-C. *J. Am. Chem. Soc.* **2001**, *123*, 8790.
(23) Campá, J. A.; Gutierrez-Puebla, E.; Monge, M. A.; Rasines, I.; Ruiz-Valero, C. *J. Solid State Chem.* **1994**, *108*, 230.
(24) Takeda, Y.; Kanno, R.; Takada, T.; Yamamoto, O.; Takano, M.; Bando, Y. *Z. Anorg. Allg. Chem.* **1986**, 259.
(25) Takeda, Y.; Kanno, R.; Takada, T.; Yamamoto, O.; Takano, M.; Bando, Y. *Z. Anorg. Allg. Chem.* **1986**, 540.
(26) Rodriguez, J.; Gonzalez-Calbet, J.; Grenier, J. C.; Pannetier, J.; Anne, M. *Solid State Commun.* **1986**, *62*, 231.
(27) Battle, P. D.; Gibb, T. C.; Steel, A. T. *J. Chem. Soc., Dalton Trans.* **1988**, 83.

The actual structures of these trigonal and rhombohedral compounds $A_{1+x}(A'_xB_{1-x})O_3$ deviate considerably from the ideal layer description. The main cause of this deviation is the fact that the A′ site coordination forces a height for the $A'O_6$ trigonal prisms, which is much smaller than the ideal c_{2H} value, being typically about $0.7-0.8c_{2H}$. Consequently, the $[A'B]O_3$ chains acquire their own length scale, which *competes* with the one coming from the stacking layer picture. One can talk then of a composite with two subsystems. This alternative viewpoint is quite efficient for interpreting the diffraction diagrams in the case of materials with long *c* parameters. Thus, their quantitative analysis is usually done by treating them as *modulated composites*, either commensurate or incommensurate.[9,13−15,19−22] The structure is then depicted as two mutually interacting subsystems modulated along *z* with two different average periodicities, but periodic on the plane *xy*. Subsystem 1 is formed by the $[A',B]O_3$ chains and has an average *c* parameter c_1 close to $c_{2H}/2$, while the average structure of subsystem 2, formed by the A cations, has a *c* lattice parameter $c_2 \approx c_{2H}$. The average unit cell of the [A] subsystem contains twice as many "molecular" units as the average cell of the $[A',B]O_3$ subsystem. Hence, the composition of a given compound can be directly related to the ratio of the *c* parameters of the two average substructures. A mere determination of the ratio $\gamma = c_2^*/c_1^* = c_1/c_2$, directly observable in a diffraction photograph, is sufficient for deriving the compound composition *x* through the relation $\gamma = (1 + x)/2$.[5,14,15] According to the range of values of *x*, the parameter γ can vary between 1/2 and 3/4. This composite picture stresses the chainlike 1-dimensional features of these systems. The structures are then solved using the so-called *superspace* formalism, which uses, as a very efficient mathematical tool, a one-to-one correspondence between the experimental 3-dimensional structure and an abstract mathematical periodic structure defined in a (3+1)-dimensional space.[29] The superspace group is rhombohedral ($R\bar{3}m(00\gamma)0s$) with an *a* parameter of around 10 Å ($\sqrt{3}a_{2H}$). In the commensurate case, the conventional symmetry of the structure is either trigonal or rhombohedral with a superstructure *c* parameter (common multiple of c_1 and c_2) that depends on the composition.

Although the composite-modulated description is the one usually employed in the quantitative analyses of these structures, one can alternatively apply the superspace tools while maintaining a layer picture of the structure and using the ideal layer model as the reference structure. The experimental structure is then described as a modulated structure whose occupational modulation defines a particular stacking of perfect ideal layers of type $A_3A'O_6$ and A_3O_9, plus some *displacive* modulations which deviate the atoms from their idealized layer positions.[11,30] We have recently demonstrated the full equivalence of both approaches for this rhombohedral series, that is, the equivalence of the description as a modulated composite or as a layered modulated structure (with a single average structure).[30] An alternative general formula of the series, which is better adapted to the modulated layer model, expresses the compound composition in the form $A(A'_yB_{1-2y})O_{3(1-y)}$, where $y = n/3(n + m) = x/(1 + x)$. The parameter *y* corresponds to one-third of the proportion of substituted layers of type $A_3A'O_6$ in the total layer sequence. This generic formula uses the A cations (the only cations equally present in all layers, as reference composition) and makes the substitution of three oxygens by the cation A′ explicit. The composition limits of the family now correspond to $y = 0$ and $y = 1/3$.

The Ba−Co−O system is particularly rich in phases belonging to this family.[16,17] The Co acts in these compounds both as the B cation with octahedral coordination and as the A′ cation within the trigonal prisms. The phases $Ba_9Co_8O_{24}$ ($x = 1/8$), $Ba_8Co_7O_{21}$ ($x = 1/7$), $Ba_{15}Co_{13}O_{39}$ ($x = 2/13$), and $Ba_{66}Co_{59}O_{177}$ ($x = 7/59$) have been studied by electron diffraction and high-resolution electron microscopy.[16,17] Recently, the structure of $Ba_{1.1064}CoO_3$ has been solved on a single crystal using the supespace formalism.[31] The composition is very close to the member $n = 3$, $m = 7$ ($x = 1/9$), which corresponds to the sequence of one trigonal prism plus eight octahedra along the chains.

The structure determination of these compounds and many others of this family has shown that the sequence of octahedra and trigonal prisms along each $[A'B]O_3$ chain, their correlated positions along neighboring chains, and the layer stacking sequences as a function of the *x* composition follow simple but very restrictive rules. They essentially imply a space distribution of the minority trigonal prisms as uniformly as possible. When seen as a layered structure, this implies that the stacking sequence realized at each composition is the one which distributes the $A_3A'O_6$ layers in the most uniform way.[30]

Recently, within the Ba−Co−O system, a new series of structures also related to the 2H-hexagonal perovskite has been discovered and a preliminary characterization by electron diffraction and high-resolution electron microscopy has been reported.[32,33] The members $Ba_8Co_7O_{21}$, $Ba_9Co_8O_{24}$, $Ba_{10}Co_9O_{27}$, $Ba_{11}Co_{10}O_{30}$, and $Ba_{12}Co_{11}O_{33}$ have been isolated.[32,33] All of these phases have been indexed according to an orthorhombic unit cell with an *a* parameter around 11.4 Å ($\approx 2a_{2H}$), $b \approx 19.8$ Å ($2\sqrt{3}a_{2H}$), and a *c* parameter depending on the composition. As for the rhombohedral series, the layer stacking is hexagonal and the general formula can also be expressed as $A_{1+x}(A'_xB_{1-x})O_3$ (composite) or $A(A'_yB_{1-2y})O_{3(1-y)}$ (modulated layer model), but the layers involved are different. In this case, the stoichiometry of the phases results from the stacking of A_8O_{24} layers ($4 \times AO_3$) and $A_8A'_2O_{18}$ layers. The general formula of the series can be written as $A_{4m+4n}A'_nB_{4m+2n}O_{12m+9n}$ where m/n is the proportion of $[A_8O_{24}]$ and $[A_8A'_2O_{18}]$ layers in the sequence. The $[A_8A'_2O_{18}]$ layers result from the normal close-packed $[A_8O_{24}]$ layers by an ordered re-

(28) Harrison, W. T. A.; Hegwood, S. L.; Jacobson, A. J. *J. Chem. Soc., Chem. Commun.* **1995**, 1953.
(29) Janssen, T.; Janner, A.; Looijenga-Vos, A.; de Wolf, P. M. *Tables for Crystallography*; Wilson, A. J. C., Ed.; Kluwer Academic Publishers: Dordrecht, 1992; p 797.
(30) Elcoro, L.; Darriet, J.; El Abed, A.; Perez-Mato, J. M., to be published.
(31) El Abed, A.; Elqebbaj, S. E.; Zakhour, M.; Champeaux, M.; Perez-Mato, J. M.; Darriet, J. *J. Solid State Chem.* **2001**, *161*, 300.
(32) Boulahya, K.; Parras, M.; Gonzalez-Calbet, J. M. *Chem. Mater.* **2000**, *12*, 2727−2735.
(33) Boulahya, K.; Parras, M.; Gonzalez-Calbet, J. M. *J. Solid State Chem.* **2000**, *151*, 77−84.

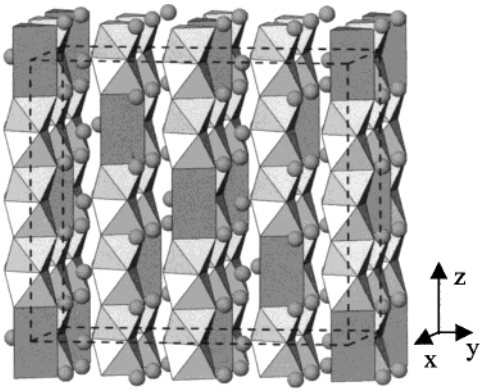

Figure 3. Schematic representation of the ideal layer model for the orthorhombic structure of $Ba_8Co_7O_{21}$.

moval (two times per A_8O_{24}) of groups of three oxygen atoms replaced by an A′ atom.[32,33] These two types of layers are represented in Figure 1a,c and their relationship with the AO_3 and $A_3A'O_6$ layers are outlined. The basic principle is similar to that, giving rise to the $A_3A'O_6$ layer, but now the stoichiometry of the layer is different. Here again, the structures can be described as a set of $[A'B]O_3$ chains parallel to the *c* axis separated by the A atoms and formed by trigonal prisms ($A'O_6$) and octahedra (BO_6) in the proportion $p/(q - p)$ for $x = p/q$ (p, q integers). The lattice periodicity of the chains on the *xy* plane changes, however, to an orthorhombic or pseudo-orthorhombic C-centered cell (see Figure 3).

This new orthorhombic series has a close relationship with the well-studied rhombohedral series mentioned above. Following the same general principles empirically observed in the rhombohedral series, we propose a unique superspace model for this new orthorhombic series.[30] As in the rhombohedral case, if correct, this model can in principle be used for refining any of these structures with high accuracy, avoiding the problems of a conventional crystallographic approach (conventional crystallographic methods are normally inefficient because of the typically large values of the *c* unit cell parameter and the strong correlations between the atomic positions which cannot be described by conventional crystallographic symmetry). As a byproduct, this postulated superspace model predicts for any composition the layer-stacking sequence and the $[A'B]O_3$ chain configurations in terms of octahedra and trigonal prisms, together with the conventional space group of the structure. It is then striking that some of the proposals about layer-stacking sequences and chain configurations coming from the first characterization of these compounds by electron diffraction and high-resolution electron microscopy[32] are at variance with this model. If this early report were fully correct, some of these structures, and in particular $Ba_{12}Co_{11}O_{33}$, would not follow the general principle of uniform distribution of minority motifs observed in the rhombohedral series, which are the basis of the unifying description of these materials within a single superspace model. It seems, therefore, important to carry out a quantitative investigation of the structure of some of these phases using single-crystal X-ray diffraction techniques to establish a comparison with the rhombohedral series under sure experimental basis.

In this paper we report the structure determination from single-crystal X-ray diffraction data of the compound $Ba_{12}Co_{11}O_{33}$, belonging to the series ($x = 1/11$, $y = 1/12$). We will show that indeed this system follows a layer-stacking sequence consistent with the rules observed in the rhombohedral series. Furthermore, the structure refinement could be successfully performed with the superspace model proposed and postulated by analogy with the rhombohedral series.[30] Hence, at least for this compound, the preliminary model proposed from electron microscopy images[32] can be disregarded.

The paper is organized as follows: first, a summary of the structural properties of the compounds of the rhombohedral series, regarding the configuration of the $[A'B]O_3$ chains and the layer-stacking sequences, and its extrapolation to the new "orthorhombic" series is given. The compatibility with these empirical general rules of the structural models proposed in previous literature is then discussed. Next, the superspace model, which, by analogy with the rhombohedral series, is expected to be valid for the whole series, is outlined. This model is first presented maintaining a layered picture of the structure where the two types of layers, A_8O_{24} and $A_8A'_2O_{18}$, are emphasized. The equivalent model within the modulated composite picture is also given. Finally, the structure of $Ba_{12}Co_{11}O_{33}$ is solved using both superspace models, demonstrating their equivalence. The resulting 3-dimensional structure is then discussed.

2. Layer-Stacking Rules

In the rhombohedral series, the sequence of octahedra and trigonal prisms along each $[A'B]O_3$ chain and their correlated positions along neighboring chains follow the simple but very restrictive principle that the distribution of the minority trigonal prisms should be as uniform as possible. Thus, along the chains, the sequences of octahedra and prisms are so-called "uniform"[34] and can be derived for each composition by the simple means of locating the fraction *x* in a Farey tree.[5] Thus, for instance, for $x = 1/10$, one would have along the chains a sequence of 9 octahedra and 1 trigonal prism (9Oh−1Tp), or in short ⟨91⟩, and not, for instance, a sequence 8Oh−1Tp−10Oh−1Tp (in short ⟨(81)((10)1)⟩), which would have the same composition but is not *uniform*. More complex sequences appear when the numerator of *x* is not unity. Thus, for $x = 2/11$, as this fraction is generated in the Farey tree from 1/5 and 1/6 [$2/11 = (1 + 1)/(5 + 6)$], the uniform sequence is ⟨(41)(51)⟩ (or 4Oh−1Tp−5Oh−1Tp), that is, a juxtaposition of the sequences corresponding to $x = 1/5$ and $x = 1/6$.[20] For each composition, there is only one possible uniform sequence, which can be quite complex. For example, in the case $x = 13/81$, the sequence ⟨$(51)^4(61)$-$(51)^3(61)(51)^3(61)$⟩ is realized,[13] where the exponent indicates the number of times the corresponding block is repeated consecutively. Notice that new types of isolated and uniformly distributed *minority* motifs appear (the block (61) in this case), following a kind of recursive scale hierarchy so that one can talk of the *intergrowth* of intergrowths and so on.

The locations of the trigonal prisms on neighboring chains are also scattered, following some kind of uni-

(34) Amelinckx, A.; Van Dyck, D. *Electron Diffraction Techniques*; IUCr Monographs on Crystallography 4; Oxford University Press: London, 1993; Vol. 2, p 309.

formity principle implicit in the superspace symmetry relations between the chains. This uniform distribution on the plane *xy* can be better analyzed when a layer description of the structure in terms of A_3O_9 and $A_3A'O_6$ layers in the proportion m/n ($A_{3n+3m}A'_nB_{3m+n}O_{9m+6n}$) is used. Then, it can be seen that the stacking sequence realized at each composition is the one which distributes the $A_3A'O_6$ layers in the most uniform way, keeping a hexagonal stacking and the complete equivalence between the three types of $A_3A'O_6$ layers. Thus, for the simple case of equal numbers of A_3O_9 and $A_3A'O_6$ layers ($n = m = 1$), the stacking layer sequence will be $\langle 11 \rangle_L$, that is, a sequence of 1[A_3O_9]-1[$A_3A'O_6$] layers (we use the L subindex to differentiate these layer sequences from those mentioned above for the octahedra and trigonal prisms). The stacking period is then obtained by repetition of this layer sequence, changing consecutively the three types of [$A_3A'O_6$] layers, until an actual period is attained. Thus, the stacking period is AB_1AB_2-AB_3 or the equivalent one $BA_1BA_2BA_3$, where A and B designate, as usual, the two standard types of A_3O_9 layers in the hexagonal stacking and a subindex $i = 1$, 2, 3 is used in the case of the $A_3A'O_6$ layers to distinguish between the three different layers of this type which are related by an origin shift on the plane *xy* (see Figure 1b). Similarly, if $m = 1$ and $n = 2$, we have then a sequence $\langle 12 \rangle_L$ with a period of 18 layers following the pattern $AB_1A_2BA_3B_1AB_2A_3BA_1B_2AB_3A_1$-$BA_2B_3$. In the inverse situation, for $m = 2$ and $n = 1$, the sequence between A_3O_9 and $A_3A'O_6$ layers is $\langle 21 \rangle_L$ yielding a period of 18 layers in the form ABA_1BAB_2-$ABA_3BAB_1ABA_2BAB_3$. In a more general complex case, we can again derive the uniform layer sequence using the Farey tree for the fraction $n/(n + m)$. For instance, for $n = 3$ and $m = 5$, as $3/8 = 1/3 \oplus 1/3 \oplus 1/2$, in the sense of the Farey tree, the sequence is to be $\langle (21)^2(11) \rangle_L$, that is, a sequence of two consecutive blocks corresponding to the case $n = 1$, $m = 2$ ($n/(n + m) = 1/3$) plus a block corresponding to $n = 1$, $m = 1$ ($n/(n + m) = 1/2$). The actual layer-stacking period would then be ABA_1BAB_2-AB_3, or other equivalent ones ($BAB_1ABA_2BA_3$, ABA_2-BAB_3AB_1, etc.), which will be related by twinning.[5,35]

The new *orthorhombic* series can be formulated as $A_{4m+4n}A'_nB_{4m+2n}O_{12m+9n}$, where m/n is the proportion of A_8O_{24} and $A_8A'_2O_{18}$ layers in the structure. The two limits are $m/n = 8$ corresponding to the 2H-hexagonal perovskite and $m/n = 0$, which corresponds to the case $A_4A'B_2O_9$, where all of the layers have the $A_8A'_2O_{18}$ composition. When expressed in the general form $A_{1+x}(A'_xB_{1-x})O_3$, x takes the value $n/(4m + 3n)$. In this formulation, the composition x can be any number between 0 and 1/3. The composition x is related to the proportion of trigonal prisms and octahedra along the [A′B]O_3 chains in the same form as in the rhombohedral series. If the value of x is p/q (p, q integers), p represents the number of trigonal prisms and $(q - p)$ the number of octahedra in the sequence along the columns. One can then expect that these orthorhombic compounds will also exhibit uniform sequences of octahedra and prisms along the chains. When expressed in the layerlike formulation $A(A'_yB_{1-2y})O_{3(1-y)}$, the value of y in this case is $y = n/4(n + m) = x/(1 + x)$, that is, one-fourth of the proportion of substituted layers of type $A_8A'_2O_{18}$ in the layer sequence. The composition limits of the family correspond in this case to $y = 0$ and $y = 1/4$.

Table 1. Atomic Coordinates of $Ba_8Co_7O_{21}$ in a Perfect Rigid Model

atom	site	*x*	*y*	*z*	atom	site	*x*	*y*	*z*
Ba1	8a	0	1/6	0	O2	16b	1/8	7/24	0
Ba2	8a	1/2	1/6	0	O3	16b	3/8	7/24	0
Ba3	16b	1/4	5/12	0	O4	16b	1/4	1/6	0
Ba4	16b	1/4	1/12	1/8	O5	16b	3/8	1/24	0
Ba5	16b	3/4	1/12	1/8	O6	16b	0	1/12	1/8
Co1	8a	0	0	0	O7	16b	1/2	1/12	1/8
Co2	16b	0	0	3/16	O8	16b	1/8	5/24	1/8
Co3	16b	0	0	5/16	O9	16b	3/8	5/24	1/8
Co4	16b	0	0	7/16	O10	16b	5/8	5/24	1/8
O1	8a	0	5/12	0	O11	16b	7/8	5/24	1/8

One can generalize the *uniform* stacking rules observed in the rhombohedral series to this new series in a straightforward manner. The number of distiguishable $A_8A'_2O_{18}$ layers, which depends on the position of the A′ cations, is four (see Figure 1c). The uniform sequences of layers for each composition can be constructed in a analogous way as above. For instance, for $m = n = 1$ ($Ba_8Co_7O_{21}$), the global-type layer sequence should be $\langle 11 \rangle_L$ and because there are four distinguishable layers for the $A_8A'_2O_{18}$ type, the resulting stacking period will be $AB_1AB_2AB_3AB_4$ (or equivalent). The [A′B]O_3 chains will then follow a sequence of 6Oh−1Tp ($\langle 61 \rangle$), as should be for a uniform sequence in the chain configuration.

$Ba_8Co_7O_{21}$ is in fact the first compound belonging to this series that has been synthesized and characterized.[33] The unit-cell parameters are $a = 11.48(3)$ Å, $b = 19.89(4)$ Å, and $c = 17.46(6)$ Å.[33] The relation of these parameters with those of the 2H-hexagonal perovskite ($a_{2H} = b_{2H}$ and c_{2H}) are as follows: $a = 2a_{2H}$, $b = 2a_{2H} + 4b_{2H}$, and $c = 4c_{2H}$. The symmetry was identified as orthorhombic with the space group *Fd*2*d*. An ideal layered structural model of $Ba_8Co_7O_{21}$ was also proposed in ref 33 from the comparison of simulated and high-resolution electron microscopy images. Although the proposed model follows the expected stacking sequence predicted above (Figure 3), the corresponding ideal atomic coordinates (Table 2 in ref 33) are clearly wrong. These atomic coordinates are supposed to be derived from a perfect rigid layer model where the height of the trigonal prism along the *c* axis is twice the height of the octahedron, and the layers are equidistant along the *c* parameter. The table presents in fact duplicated (symmetry-equivalent) positions and yields incorrect interatomic distances. For further reference we present in Table 1, a correct list of independent atomic positions for this idealized layered model of $Ba_8Co_7O_{21}$ with *Fd*2*d* symmetry.

In the case of the compound investigated here, Ba_{12}-$Co_{11}O_{33}$, having $m = 2$ and $n = 1$ ($y = 1/12$), we expect a sequence of type $\langle 21 \rangle_L$ and a resulting stacking period of 12 layers $ABA_1BAB_2ABA_3BAB_4$ (or equivalent), yielding [CoO_3]chains with sequences of 10Oh−1Tp. The model for this compound proposed in ref 32 from the analysis of high-resolution electron microscopy images is clearly incompatible with the stacking sequence indicated above. It includes the intergrowth of two 2H normal blocks. The presence of normal 2H slabs along *c* requires the presence of at least three consecutive normal Ba_8O_{24} layers, which according to the *uniform*

(35) Gourdon, O.; Cario, L.; Petricek, V., Perez-Mato, J. M.; Evain M. *Z. Kristallogr.* **2001**, *216*, 541−555.

stacking rules extrapolated from the rhombohedral series would only appear for compositions with $m/n > 2$ ($y < 1/12$).

In fact, except for the initial $Ba_8Co_7O_{21}$,[33] all the structural models proposed in ref 32 for the rest of the compounds in the series investigated ($Ba_{10}Co_9O_{27}$, $Ba_{12}O_{11}O_{33}$, $Ba_9O_8O_{24}$, and $Ba_{11}Co_{10}O_{30}$) are in contradiction with the principle of uniform stacking sequences observed in the rhombohedral series. An accurate structure determination of these compounds is therefore necessary to contrast this apparent exceptional behavior. In the following, we report a single-crystal X-ray structure determination of $Ba_{12}O_{11}O_{33}$. We already advance that the obtained structure does not confirm these early reports and is in fact fully consistent with the principles observed in the rhombohedral series. The layers follow the *uniform* stacking sequence, which corresponds to its composition, as discussed above. This refutes the preliminary model from ref 32.

3. Superspace Model

In the superspace description, the above-discussed general principle of *uniformity* for the layer stacking in intergrowth polytypoids translates into the existence of a single common structural model for the whole series, which is essentially independent of composition, except for the change of the modulus of the modulation wave vector.[36−38] In this common superspace model, the average structure has a unit cell with c_{2H} as the c parameter, while on the plane xy, the cell parameters are those of the mixed layers $A_8A'_2O_{18}$ ($a = 2a_{2H}$, $b = 2a_{2H} + 4b_{2H}$). The *atomic domains* along the internal space, which represent the atomic positions realized in real space, have relative positions that satisfy a steric condition analogous to the so-called *closeness condition* considered in the modelization of quasicrystals.[39,40] This automatically yields uniform sequences for any composition. The superspace model also contains the symmetry features common to the whole family and allows the prediction of the conventional space group symmetry for any composition.[5,14,36−38]

In Figure 4a a scheme is depicted of the layer configuration for a generic compound $Ba(Co_{1-y})O_{3(1-y)}$ of the orthorhombic series as described in superspace according to the rules observed for the rhombohedral series.[30] This type of sceme is similar to those proposed in refs 36−38. The figure represents a projection of the ideal layer atomic positions on the plane x_3x_4. Each domain parallel to x_4 depicted in the figure corresponds to an ideal layer type; that is, in this domain all atomic occupation domains associated with all atoms of the layer of the type indicated (having different x (x_1), y (x_2) coordinates but equal z (x_3) coordinates) superpose. The widths of the layer domains are forced by the compound composition, that is, the relative ratio of each type of layer in the structure. As the proportion of $Ba_8Co_2O_{18}$ layers should be $n/n + m$, each domain for a given layer of type A_i (B_i) has along x_4 a width $\Delta_s = n/4(n + m) = y$. The remaining intervals along x_4 are occupied by normal A(B) Ba_8O_{24} layers. The modulation wave vector $q_L = \gamma_L c_{2H}^*$ assigned to the structure is such that any two $Ba_8Co_2O_{18}$ layers of the same numeric type, A_i and B_i, are as far apart as possible; that is, their domains when projected on x_4 just juxtapose without overlap. This is analogous to the so-called *closeness condition* in quasicrystals.[39,40] In the present case, this condition is achieved with $\gamma_L = 2\Delta_s = 2y$, forcing a one-to-one relationship between the modulation wave vector and composition. The actual atomic positions of the real space structure are given by a horizontal section of the 4-dimensional periodic structure whose x_3x_4 unit cell projection is shown in the figure. Therefore, by construction, the layers stack along z according to an AB hexagonal sequence separated by a distance $\approx c_{2H}/2$, and the type of layer in each case (a normal Ba_8O_{24} layer or a $Ba_8Co_2O_{18}$ layer of type 1, 2, 3, or 4) will depend on which of the layer domains is being cut by the horizontal real z axis. In Figure 4b,c, the way the layer stacking sequences are derived from the superspace model is shown for two different values of y (1/12 and 2/9). As expected, the sequences are equivalent to those resulting from the rules discussed in the previous section.

Obviously, the consecutive 1−4 label numbers associated with the four types of A_i and B_i layers are arbitrary and one can wonder if there is anything particular in the consecutive ordering of the four-layer intervals along x_4 or if other alternative orderings would yield equally valid models. In fact, some of them give equivalent layer sequences, yet others give different (nonequivalent) layer sequences, also having different superspace groups.[30] The model proposed here is the construction that has the highest superspace symmetry and distributes the prismatic cations in the most uniform way throughout the whole space. The final refinement of the structure will demonstrate the correctness of this choice.

Up to now, we have only considered the Ba_8O_{24} and $Ba_8Co_2O_{18}$ close-packed layers. The Co cations not belonging to the latter will form intermediate layers occupying the octahedral interstices in between. The number of these interstices and their location depend on the type of the two adjacent layers. We can then distinguish three different types of intermediate Co layers depending on the type of their neighboring close-packed layers: layers with eight, six, and four Co octahedral sites, depending on whether the Co layer is between two [A_8O_{24}] layers, a [A_8O_{24}] and a [$A_8A'_2O_{18}$] layer, or two [$A_8A'_2O_{18}$] layers, respectively. In the uniform sequences represented by the superspace model in Figure 4b, $y < 1/8$ ($n < m$), there are no successive [$A_8A'_2O_{18}$] layers. In the superspace the different *layer coordinations* for the Co octahedral cations realized along the layer sequence can be easily retrieved by looking at different horizontal sections of the superspace unit cell. One can then easily distinguish continuous intervals along x_4 corresponding to different types of consecutive close-packed layers. Figure 4d shows the particular case of $y = 1/12$. Each interval corresponds to a type of Co layer.

(36) Elcoro, L.; Perez-Mato, J. M.; Withers, R. L. *Z. Kristallogr.* **2000**, *215*, 727−739.
(37) Elcoro, L.; Perez-Mato, J. M.; Withers, R. L. *Acta Crystallogr.* **2001**, *B57*, 471−484.
(38) Boullay, P.; Trolliard, G.; Mercurio D.; Perez-Mato, J. M.; Elcoro, L. (Part I and II) *J. Solid State Chem.* **2002**, *164*, 252−260.
(39) Cornier-Quiquandon, M.; Gratias, D.; Katz, A. *Methods of Structural Analysis of Modulated Structures and Quasicrystals*; Perez-Mato, J. M., Zúñiga, F., Madariaga, J., G., Eds.; World Scientific: Singapore, 1991; pp 313−332.
(40) Katz, A.; Gratias, D. *J. Non-Cryst. Solids* **1993**, *187*, 153−154.

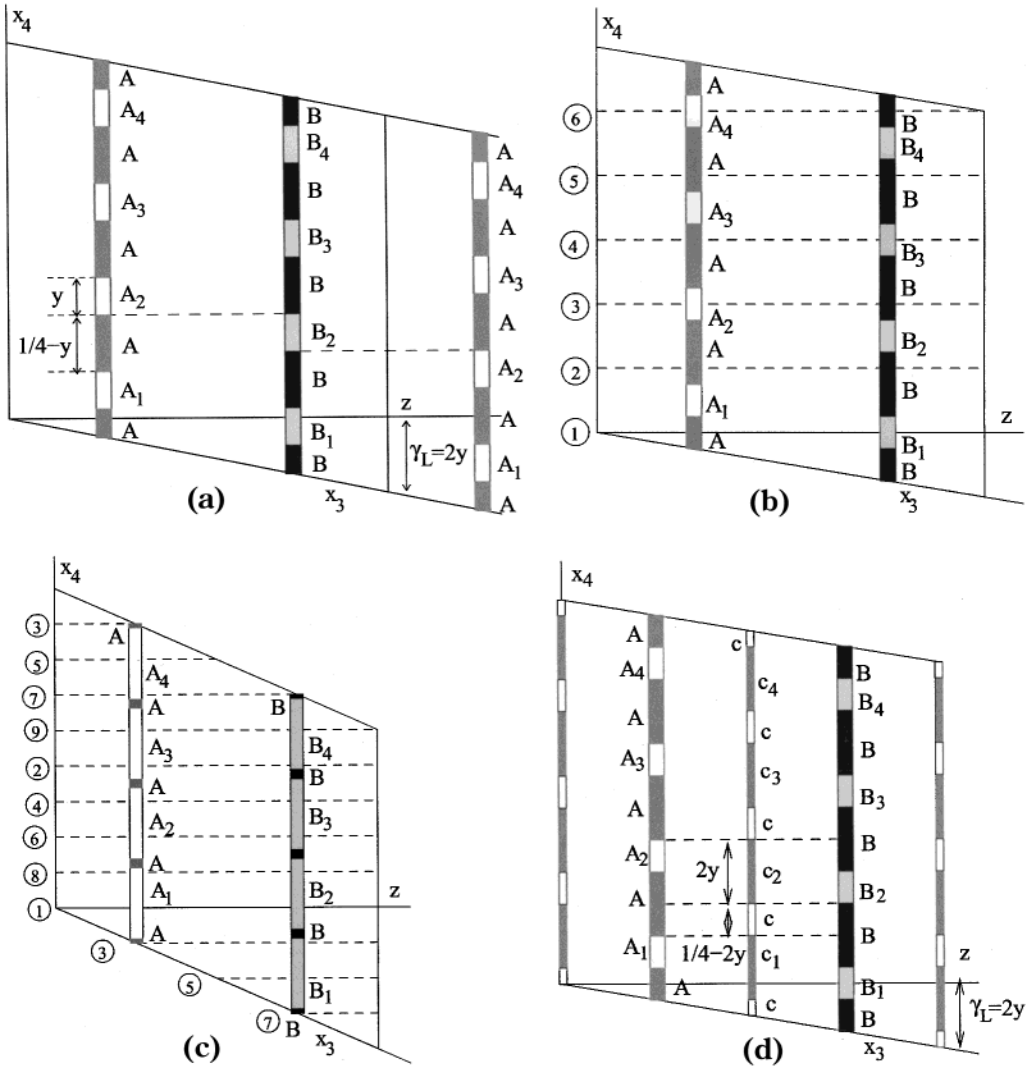

Figure 4. (a) (x_3,x_4) projection of the domains in superspace corresponding to the layers of type A, B, A_i, and B_i (i = 1, 2, 3, 4) for the idealized layer model of an orthorhombic $A(A'_yB_{1-2y})O_{3(1-y)}$ compound. (b) and (c) represent the same projection for the particular commensurate compositions y = 1/12 and y = 2/9, respectively. The resulting layer sequences ($AB_1ABA_2BAB_3ABA_4B$ and $A_1B_2A_3B_4AB_1A_2B_3A_4B_1A_2B_3A_4BA_1B_2A_3B_4$, respectively) are graphically obtained. (d) The same superspace projection as in (a) including the domains representing the interstitial layers of Co.

From the 3-dimensional symmetry of the ideal real space layers and their location in the superspace unit cell, the superspace symmetry of the global ideal 4-dimensional configuration can be derived. This is given by the superspace group $Xdcd(00\gamma_L)qq0$, where X represents a nonconventional centering according to the translations (1/2, 1/2, 0, 0), (1/2, 0, 0, 1/2), and (0, 1/2, 0, 1/2). The full set of symmetry operations defining this group are given in Table 2. This group is equivalent to the superspace group $Pbnn(1/2\ 1/2\ \gamma_L)qq0$ with $a' = a/2$, $b' = b/2$, and $c' = c$ average unit cell (No. 52.7 from the list in volume C of the *International Tables for Crystallography*[29]). For commensurate values of γ_L, or in practice, for simple fractional values of x, the actual symmetry of the compound can also be described by a conventional space group with a superstructure Bravais lattice. The possible space groups in each case can be directly derived from the superspace group and are listed in Table 3. They depend on the type of fraction $\gamma_L = 2x/(1 + x)$ and the x_4 section, which is taken as real space. Table 3 considers all possible space group symmetries for a commensurate structure with continuous atomic domains. In our case, however, some of the listed space groups correspond to x_4 sections that pass just through one or more of the borders between intervals corresponding to different layers. At these isolated mathematical points some occupation functions are discontinuous and the model has less symmetry than the one expected for a modulated structure with continuous functions. Consequently, some of the space

Table 2. Generators and Centering Translations of the Superspace Groups $Xdcd(00\gamma_L)qq0$ (Layer Option) and $Fddd(00\gamma_C)0s0$ (Composite Option) and Resulting Reflection Conditions[a]

$Xdcd(00\gamma_L)qq0$ superspace group	$Fddd(00\gamma_C)0s0$ superspace group
x_1, x_2, x_3, x_4	x_1, x_2, x_3, x_4
$-x_1, {}^1/_4 + x_2, x_3, {}^1/_4 + x_4$	$-x_1, {}^1/_4 + x_2, {}^3/_4 + x_3, x_4$
${}^1/_4 + x_1, -x_2, {}^1/_2 + x_3, {}^1/_4 + x_4$	${}^1/_4 + x_1, -x_2, {}^3/_4 + x_3, {}^1/_2 + x_4$
${}^1/_4 + x_1, {}^1/_4 + x_2, {}^1/_2 - x_3, -x_4$	${}^1/_4 + x_1, {}^1/_4 + x_2, -x_3, {}^1/_2 - x_4$
reflection conditions:	reflection conditions:
$(h\ k\ l\ m)\ h + k$ = even	$(h\ k\ l\ m)\ h + k$ = even
$(h\ k\ l\ m)\ h + m$ = even	$(h\ k\ l\ m)\ h + l$ = even
$(0\ k\ l\ m)\ k + m$ = 2*even	$(0\ k\ l\ m)\ k + 3l$ = 2*even
$(h\ 0\ l\ m)\ h + 2l + m$ = 2*even	$(h\ 0\ l\ m)\ h + 3l + 2m$ = 2*even
$(h\ k\ 0\ 0)\ h + k$ = 2*even	$(h\ k\ 0\ 0)\ h + k$ = 2*even

[a] They are equivalent to $Pbnn(00\gamma_L)qq0$ (No. 52.7) and $Fddd(00\gamma_C)s00$ (No. 70.2) superspace groups in the *International Tables for Crystallography*,[29] respectively.

Table 3. Space Groups for Commensurate Structures with Rational Modulation Parameter $\gamma_L = r/s$, t Parameter, and Superspace Group $Xdcd(00\gamma_L)qq0$ (Layer Option) and $\gamma_C = r'/s'$ with t' Parameter and Superspace Group $Fddd(00\gamma_C)0s$ (Composite Option)[a]

$s = 4n$	$t = 0$ (mod. 1/2s)	$t = 1/4s$ (mod. 1/2s)	t = arbitrary
$r' = 4n$	$t' = 0$ (mod. 1/2s')	$t' = 1/4$ (mod. 1/2s')	t' = arbitrary
	*$F2/d11$ (No. 15)	$Fd2d$ (No. 43)	$Fd11$ (No. 9)
$s = 4n + 2$	$t = 0$ (mod. 1/2s)	$t = 1/8$ (mod. 1/2s)	t = arbitrary
$r' = 4n + 2$	$t' = 0$ (mod. 1/2s')	$t' = 1/4$ (mod. 1/2s')	t' = arbitrary
	$F12/d1$ (No. 15)	*$F2dd$ (No. 43)	$F1d1$ (No. 9)
s = odd	$t = 0$ (mod. 1/4s)	$t = 1/8$ (mod. 1/4s)	t = arbitrary
r' = odd	$t' = 0$ (mod. 1/4s')	$t' = 1/8s$ (mod. 1/4s')	t' = arbitrary
	$C112_1/d$ (No. 14)	*$C222_1$ (No. 20)	$C112_1$ (No. 4)

[a] The number in the *International Tables for Crystallography* of the resulting space group or equivalent is given. The space groups with asterisks are irrelevant for this compound series (see the text).

groups listed in Table 3 are not relevant for our model, as indicated in the table.

Obviously, the actual atomic positions in the real structure will deviate from the ideal positions that can be derived from a perfect layered model, but it is an empirical fact that in most cases the maximal symmetry associated with this idealized configuration is maintained in the real structure, and this is also in principle valid for the superspace group symmetry. According to Table 3, $Ba_8Co_7O_{21}$ (with $\gamma_L = 1/4$) should have symmetry $Fd2d$ (No. = 43) or $Fd11$ (No. = 9). This agrees with the space group $Fd2d$, which was assigned to this compound in ref 33. In the case of $Ba_{12}O_{11}O_{33}$ ($\gamma_L = 1/6$), however, the expected symmetry according to Table 3 is a monoclinic group $F12/d1$ (No. = 15) or $F1d1$ (No. 9), in contrast to the orthorhombic symmetry assumed by Boulahya et al.[32]

In the superspace construction, the location of the different intervals along x_4 corresponding to different layers is realized through the overlap of the occupation domains of the corresponding atoms described by crenel functions along x_4.[41,42] For instance, the three oxygen atoms with (x,y) positions (1/8, 5/24), (0, 1/12) and (1/4, 1/12) in a layer are present in all A layers except the ones of type A_1. This means that the occupation crenels associated with these oxygens should leave only the interval $[1/8 - y/2, 1/8 + y/2]$ unoccupied along x_4 where the layers of type A_1 are situated. This implies that the width of the atomic domains should be $\Delta = 1 - y$ with its center located at $x_4 = 5/8$. In this way, the occupation domains of all atoms, described in general by crenel functions, can be derived. Table 4 lists the resulting asymmetric unit for a structure with the generic composition y. Figure 5 schematically shows how the layer domains in superspace are realized through the overlap of the occupation domains of the individual atoms.

The superspace model of Table 4 with zero displacive modulations describes the perfect *uniform* layer model associated with each composition. The last column of the table indicates for each atomic domain the form (symmetry) of the atomic displacive modulations allowed by the superspace group. A structure determination essentially reduces these modulation functions (the modulation of the thermal displacement coefficients may also be considered) through a refinement process. As these functions are usually quite smooth or simple, they can be described with sufficient accuracy using a reduced number of parameters. Furthermore, these functions do not change much with composition and, therefore, with the period of the layer sequence. Consequently, the effective number of parameters describing these functions is expected to be essentially constant, independent of the actual size of the conventional unit cell. For large unit cells this number is usually significantly lower than that in a conventional superstructure refinement. This is the main advantage of the superspace formalism for describing and analyzing these long-period commensurate modulated structures: an efficient minimal parametrization of the structures.

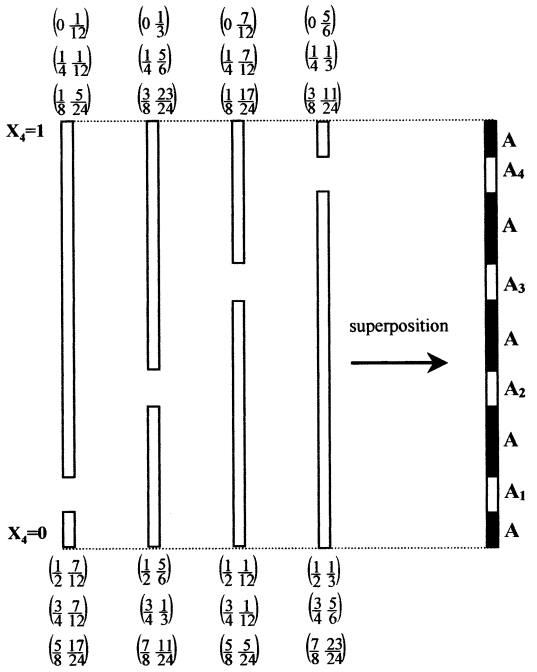

Figure 5. Scheme of how the individual atomic domains produce the layer domains in superspace. The atomic domains associated with the 24 oxygen distinct sites are depicted showing their relative position along x_4. Only four domains are distinguishable; each one represents the superposition of six O domains with different (x,y) coordinates listed in the figure. The four domains superpose in the same x_3 coordinate. The projection onto $z = x_3 = 1/4$ of the 24 atomic domains divides the $x_4 = (0,1)$ interval into A- and A_i-type domains, as shown at the right of the figure. Domains corresponding to A_i layers are defined by the vacancy of specific oxygen sites within a certain x_4 interval.

Similar to how it happens with the rhombohedral series, this orthorhombic family can be formulated as $Ba_{1+x}CoO_3$ and can be described as a modulated composite with subsystem 1 formed by the CoO_3 chains and subsystem 2 by the Ba cations. Subsystem 1 is then described as a modulated structure with the average unit cell defined by the same a and b basis vectors in the xy layer and $c_1 = c_C = \gamma_C c_L$ (main reflections $H = ha^* + kb^* + l_1c_C^*$ and modulation wave vector $q_c = \gamma_C c_C$ with $\gamma_C = (1 + x)/2$), while subsystem 2 has an average structure unit cell defined by the a, b, and $c_2 = c_C/\gamma_C = c_L$ vectors and its modulation wave vector is associated with the average period of subsystem 1. The matrix that

(41) Petricek, V.; Van der Lee, A.; Evain, M. *Acta Crystallogr.* **1995**, *A51*, 529−535.
(42) Boucher, F.; Evain, M.; Petricek, V. *Acta Crystallogr.* **1996**, *A52*, 100.

Table 4. Structural Parameters in the Superspace Description for a Compound of General Composition $A(A'_yB_{1-2y})O_3(_{1-y})$ When Described as a Layered Modulated Structure, Layer Option (Superspace Group $Xdcd(00\gamma_L)qq0$) and as a Composite ($A_{1+x}(A'_xB_{1-x})O_3$, $y = 1/(1 + x)$), Composite Option Superspace Group ($Fddd(00\gamma_C)0s0$)[a]

atom name	x_1	x_2	x_3	x_4	Δ	point symmetry	displacive modulation
B	−1/8	−1/8	0	3/8	1−2y	211	$(x_1^s(x_4), x_2^a(x_4), x_3^a(x_4))$
	[−1/8]	*[−1/8]*	*[−3/8]*	*[0]*	*[(1 − x)/2]*		
A′	−1/8	−1/8	1/4	−1/8	y	121	$(x_1^a(x_4), x_2^s(x_4), x_3^a(x_4))$
	[−1/8]	*[−1/8]*	*[−3/8]*	*[1/4]*	*[x/2]*		
O1	−1/8	−1/24	1/4	3/8	$1 - y$	121	$(x_1^a(x_4), x_2^s(x_4), x_3^a(x_4))$
	[−1/8]	*[−1/24]*	*[1/8]*	*[1/4]*	*[1/2]*		
O2	−1/4	−1/6	1/4	3/8	$1 - y$	1	$(x_1(x_4), x_2(x_4), x_3(x_4))$
	[−1/4]	*[−1/6]*	*[1/8]*	*[1/4]*	*[1/2)*		
A	−1/8	−7/24	1/4			121	$(x_1^a(x_4), x_2^s(x_4), x_3^a(x_4))$
	[−1/8]	*[−7/24]*	*[1/4]*				

[a] The parameters of the composite option are indicated in brackets below. Underlined coordinates are refinable. The fifth and sixth columns indicate the center and size of the atomic domains. In the composite option, the Co and O atoms belong to the first subsystem and the Ba atom to the second subsystem. The Ba atom in the composite option is referred to its own subsystem. The seventh column shows the point symmetry of the atomic surface and the eighth column the corresponding displacive modulation. "s", "a", and no superscripts stand for a symmetric, antisymmetric, and general function, respectively.

transforms the superspace construction from the layer picture to the composite option is

$$M = \begin{bmatrix} 1 & 0 & 0 & 0 \\ 0 & 1 & 0 & 0 \\ 0 & 0 & 0 & 1 \\ 0 & 0 & -1 & -2 \end{bmatrix}$$

so that in Table 2

$$x_i^L = \sum_j M_{ij} x_j^C$$

where x_i^L and x_i^C are the coordinates in the superspace in the layer and composite models, respectively. This matrix can be deduced from the chosen indexations of the diffraction pattern through the relation

$$h_i^L = \sum_j M_{ji} h_j^C$$

where h_i^L and h_j^C are the indicies of a reflection in the layer and composite descriptions, respectively.

Using this transformation matrix, the superspace model discussed above and summarized in Tables 2 and 3, which describes the structure as a modulated layer model, can be readily transformed into a composite model analogous to the one used in the rhombohedral series. For completeness, Tables 2 and 4 also contain the necessary information for working under this composite approach. The composite model is essentially equivalent to the one of the rhombohedral series. The relation between wave vector and composition is the same, and the crenel functions defining the occupation domains of the different atoms are also analogous. This means that for a given composition x the chains CoO_3 will exhibit the same sequence of octahedra and trigonal prisms as in the rhombohedral series. Along the z axis, the unit cell contains 8 different chains: 4 centered at $(x\ y) = (0\ 0)$, $(1/4\ 1/4)$, $(1/2\ 0)$, and $(1/4\ 3/4)$, which can be denoted as ch_1, ch_2, ch_3, and ch_4, respectively, plus their equivalent one related by the centering translation $(1/2\ 1/2\ 0\ 0)$ of the superspace group. Each pair can be denoted by the same symbol ch_i, as both translation-related chains are identical and their trigonal prisms are located at the same z value. In addition, the four chains ch_i are related by the elements of the superspace group of Table 2 for the composite option, $Fddd(00\gamma_C)0s0$. Therefore, just one of them is independent. Chains ch_1 and ch_3 are related by the centering operations $(1/2\ 0\ 1/2\ 0)$ and $(0\ 1/2\ 1/2\ 0)$ (the same happens between chains ch_2 and ch_4). Therefore, their prisms have a relative shift of 1/2 along the z axis. Finally, the sets of even and odd chains are related by the glide plane $\{m_z, -1|1/4\ 1/4\ 0\ 1/2\}$. As stressed before, the number of trigonal prisms and octahedra in each chain depends on the composition, but it is the same for all chains. As a consequence of the superspace construction and the uniformity of the layer-stacking sequence, and for any composition, the trigonal prisms are located on the different chains following the ordered sequence ch_1, ch_2, ch_3, ch_4, when moving along the stacking direction z.

In the following section we present the results of the refinement of the $x = 1/11$ ($y = 1/12$) member of the series, $Ba_{12}Co_{11}O_{33}$, using the previous superspace model, summarized in Tables 2 and 4.

4. Structure of $Ba_{12}Co_{11}O_{33}$

Single crystals were prepared by flux synthesis using a method described previously.[43] A total of 1 g of $BaCO_3$ and Co_3O_4 corresponding to the global composition $Ba_{4/3}CoO_3$ was ground and placed into an alumina crucible. Twenty grams of K_2CO_3 was packed into the crucible on top of the reagents. The crucible was covered with an alumina disk to minimize the flux evaporation. The sample was heated in air to 950 °C at 60 °C/h. The product was held at this temperature for 3 days and cooled at 6 °C/h to 880 °C. The furnace was then turned off and the system was cooled to room temperature. The crystals were washed with distilled water and dried. It is well-established that the crystals prepared by this technique are free of potassium.[43]

After several tries of checking the quality of the crystals, a very small crystal (the largest dimension was <0.05 mm) was selected and mounted on an Enraf-Nonius Kappa CCD area-detector diffractometer. Because of the dimensions of the selected crystal, no absorption corrections were made. The preliminary research of the unit cell using the Kappa CCD software led to a pseudo trigonal unit cell with $a = 11.41$ Å and $c = 27.19$ Å. The data were collected for the total sphere

(43) Hampton Henley, W.; Claridge, J. B.; Smallwood, P. L.; zur Loye, H.-C. *J. Cryst. Growth* **1999**, *204*, 122.

Table 5. Crystallogaphic Data for $Ba_{12}Co_{11}O_{33}$

(a) Data Collection

Enraf-Nonius Kappa CCD area-detector diffractometer	$a = 11.4129(2)$ Å, $c = 27.1944(6)$ Å, $\beta = 120°$
$d = 35$ mm, $t = 200$ s, $T = 293$ K	$-17 \le h \le 17$, $-17 \le k \le 17$, $-42 \le l \le 42$
Mo Kα radiation, $\theta_{max.} = 35°$	42185 measured reflections
	7902 observed reflections, $I \ge 3\sigma(I)$

(b) Data Refinement (Composite Option)

$Ba_{12/11}CoO_3$, Mr = 256.8 g	refinement on F^2, $w = 1/\sigma^2(I)$
$a = 11.4129(2)$ Å, $b = 19.7677(2)$ Å, $c_1 = 2.4722(1)$ Å, $\gamma_C = 0\ 0\ 6/11$	twin1/twin2(1/2 3/2 0, −1/2 −1/2 0, 0 0 1)/ twin3 (−1/2 −3/2 0, 1/2 −1/2 0, 0 0 1)
	0.572(2)/0.199(1)/0.229(1)
$Fddd(00\gamma_C)0s0$, $t = 0$	$R = 4.46\%$, $R_w = 8.79\%$, 4625 total reflections
$V = 557.75(2)$ Å^3, $D_x = 6.11$ g·cm^{-3}, $Z = 8$	$R = 2.48\%$, $R_w = 5.08\%$, 1419 main reflections
$\mu = 20.99$ mm^{-1}, $F(000) = 897$	$R = 6.04\%$, $R_w = 11.03\%$, 2231 satellites order 1
$R_{int.} = 2.75\%$, 7891 observed reflections, $I \ge 3\sigma(I)$	$R = 10.09\%$, $R_w = 20.31\%$, 856 satellites order 2
4625 independent reflections, $I \ge 3\sigma(I)$	$R = 30.82\%$, $R_w = 54.62\%$, 119 satellites order 3
$-17 \le h \le 17$, $-31 \le k \le 31$, $0 \le l \le 4$, $-8 \le m \le 7$	extinc. coeff. (isotropic Gaussian) 0.0085(9)
	123 refineable parameters
	$(\Delta/\sigma)_{max.} = 0.0004$, $S = 1.28$
	$\Delta\rho_{max.} = 2.50$ e Å^{-3}, $\Delta\rho_{min.} = -2.48$ e Å^{-3}

(c) Data Refinement (Layer Option)

$BaCo_{11/12}O_{33/12}$, Mr = 235.4 g	refinement on F^2, $w = 1/\sigma^2(I)$
$a = 11.4129(2)$ Å, $b = 19.7677(2)$ Å, $c_1 = 4.5324(1)$ Å, $\gamma_L = 0\ 0\ 1/6$	twin1/twin2/twin3
	0.574(3)/0.198(2)/0.228(2)
$Xdcd(00\gamma_L)qq0$, $t = 0$	$R = 4.36\%$, $R_w = 8.49\%$, 4625 total reflections
$V = 1022.5(2)$ Å^3, $D_x = 6.11$ g·cm^{-3}, $Z = 16$	$R = 2.14\%$, $R_w = 4.51\%$, 781 main reflections
$\mu = 20.99$ mm^{-1}, $F(000) = 1644$	$R = 4.87\%$, $R_w = 8.56\%$, 2482 satellites order 1
$R_{int.} = 2.75\%$, 7891 observed reflections, $I \ge 3\sigma(I)$	$R = 8.53\%$, $R_w = 17.63\%$, 1127 satellites order 2
4625 independent reflections, $I \ge 3\sigma(I)$	$R = 17.46\%$, $R_w = 32.72\%$, 235 satellites order 3
$-17 \le h \le 17$, $-30 \le k \le 31$, $0 \le l \le 7$, $-3 \le m \le 3$	extinc. coeff. (isotropic Gaussian) 0.008(1)
	151 refineable parameters
	$(\Delta/\sigma)_{max.} = 0.0008$, $S = 1.24$
	$\Delta\rho_{max.} = 3.28$ e Å^{-3}, $\Delta\rho_{min.} = -2.98$ e Å^{-3}

with $\theta_{max.} = 35°$ ($-17 \le h \le 17$; $-17 \le k \le 17$; $-42 \le l \le 42$). The measuring time was 200 s with a distance of the detector of 35 mm and a scan angle of 1°. A total of 86561 reflections were measured (Table 5). The unit cell parameters were refined using the HKL DENZO program[44] with the result $a = 11.4129(2)$ Å and $c = 27.1944(6)$ Å. The data reduction was carried out with the HKL DENZO and SCALEPACK packages,[41] yielding 42185 reflections. The set of intensities with symmetry point group 3 gives an $R_{int.} = 9.4\%$ for 4422 observed reflections ($I \ge 3\sigma$(I)). Trigonal symmetry can therefore be discarded. The model discussed above predicts instead a pseudo orthorhombic lattice with space group $F12/d1$ and $c = 6c_{2H}$ ($\gamma_L = 1/6$ or $\gamma_C = 6/11$) (see Table 3). The corresponding experimental orthorhombic unit cell (a =11.4129(2) Å, $b = a\sqrt{3} =$ 19.7177(2) Å, and $c = 27.1944(6)$ Å) was derived from the initial one through the following transformation matrix: (0 −2 0; −1 −1 0; 0 0 −1). With this unit cell, the analysis with point group 222 gives $R_{int.} = 4.31\%$ for 3467 observed reflections with $I \ge 3\sigma$(I), while for point group 2 (along the b axis) it yields 7092 observed reflections with $I \ge 3\sigma$(I) and a resulting $R_{int.}$ of 3.23. A possible twinning has been considered with respect to a 3-fold axis, related to the observed pseudo trigonal symmetry (see Table 5 for the corresponding twinning matrices). Taking into account these twin laws, all reflections agree with a F-centered space group. The data have then been analyzed separately using the two alternative descriptions: as a composite-modulated structure and as a layer model (a single modulated structure). In both approaches, a refinement process using the JANA 2000 program package[46] has been successfully accomplished.

4.1. Composite Model. In this approach the structure is considered as a misfit composite crystal with two orthorhombic subsystems with common a and b parameters but different c parameters: $a = 11.4129(2)$ Å, $b = a\sqrt{3} = 19.7677(2)$ Å, $c_1 = c/11 = 2.4722(1)$ Å, and $c_2 = c/6 = 4.5324(1)$ Å $= (c_L)$. The first subsystem related to the CoO_3 part is characterized by c_1 while the second one related to the Ba subsystem corresponds to the c_2 parameter. Both structures are modulated along z with a modulation period given by the c parameter of the other subsystem; that is, the modulation wave vector of subsystem CoO_3 is c_2^* and vice versa. The two subsystems can be analyzed separately as two independently modulated structures in direct space. However, their diffraction pattern superpose coherently in reciprocal space and then each Bragg reflection H is expressed as $H = ha^* + kb^* + lc_1^* + mc_2^*$, with $c_2^* = (6/11)c_1^*$, as expected from the general expression $c_2^*(=q_c) = \gamma_C c_1^* = (1 + x)/2c_1^*$ (see Table 2). Thus, the 4×4 W matrices[45] for each subsystem are $W_1 =$ identity and $W_2 =$ (1 0 0 0, 0 1 0 0, 0 0 0 1, 0 0 1 0), respectively, for the two indexing vectors along z. The measured (h k l) reflections referring to the orthorhombic supercell were transformed into (h k l m) indices using the JANA 2000 program package.[46] This transformation leads to 4624 independent observed reflections for $I \ge 3\sigma(I)$.

The so-called "main" reflections (h k l 0) with $l \neq 0$ and (h k 0 m) with $m \neq 0$ are interpreted as the Bragg reflections of the subsystems 1 and 2, respectively, if the modulations are neglected. In that case "authentic" satellite reflections (h k l m) with both l and $m \neq 0$ could not exist. The modulation of both systems, however,

(44) Otwinowski, Z.; Minor, W. *Methods Enzymol.* **1997**, *276*, 307.

(45) Van Smaalen, S. *Phys. Rev.* **1991**, *B43*, 11330−11341.

(46) Petricek, V.; Dusek, M., *JANA2000*; Institute of Physics, Czech Academy of Sciences: Prague, Czech Republic, 2000.

generates these satellites plus non-negligible contributions of both subsystems to the two sets of main reflections.

The CoO_3 subsystem was chosen as the reference system. The superspace group is $Fddd(00\gamma_C)0s$ ($Z = 8$) (see Table 2). As the modulation is a commensurate case, the extinction rules of the superspace group listed in Table 2 are not expected to be satisfied in general because of the ambiguity of the indexation (reflections can be indexed indistinctly with extinct and nonextinct sets of indices ($h\ k\ l\ m$)). Only the extinction rules resulting from the superstructure space group should remain. Therefore, the choice of the superspace group cannot be in principle checked through the observation of these additional superspace group extinction rules and can only be confirmed a posteriori by the success of the structure refinement. As real space, the section containing the origin $t = 0$ was taken (see Table 3). The displacive modulation functions were introduced in the refinement as Fourier series, except for the cobalt Cop corresponding to the prismatic sites where no modulation function is possible in the present commensurate case. In a commensurate case, the number of parameters defining the modulations functions in the (3+1)-dimensional option cannot exceed the number of equivalent variables in the 3-dimensional option. In our case there is only one independent position for the trigonal prism ($-1/8\ y\ -3/8$), $y \approx -1/8$, in the 3-dimensional description and, therefore, no displacive modulation should be considered for this atom. The unique independent position of the barium atom in the average structure is at ($-1/8\ y\ 1/4$) with $y \approx -7/24$. The atomic displacive modulations of Ba were also refined as a Fourier series.

The first stage of the refinement was carried out considering first-order Fourier amplitudes for the octahedral cobalt (Co), the barium, and the two oxygen atoms O1 and O2. The residual factor decreased to 15.4%. In successive steps, higher orders of the Fourier series were introduced for barium (fourth order), oxygen (third order), and cobalt (Co) (third order). The residual factor dropped to $R = 8.4\%$. In a final step, modulations of the atomic displacement parameters up to third order for Ba and first order for Co and O were included in the refinement. Then, the final residual factor R stabilized at 4.46% for 123 independent refined parameters (Table 5). The final atomic positional and atomic displacement parameters defining the atomic domains and their modulation functions are gathered in Table 6.

The variation of the z-fractional coordinates of the CoO_3 and Ba subsystems versus the internal coordinate t ($t = x_4 - q_C \cdot r_{av.}$) are given in Figures 6 and 7, respectively. Because it is a commensurate structure, the discrete points (squares and circles) in Figure 6 correspond to the positions realized in the CoO_3 chain located at $x \approx y \approx 7/8$. The other CoO_3 chains are related to that one by symmetry. The fractional atomic positions of the resulting 3-dimensional structure (space group $F12/d1$, equivalent to No. 15 in the *International Tables for Crystallography*,[29] unit-cell parameters $a = 11.4129$ Å, $b = 19.7677$ Å, $c = 11c_1 = 6c_2 = 27.1942$ Å, $\alpha = \beta = \gamma = 90°$ (b unique)) described in a conventional form are given in Table 7. These atomic positions correspond to the section $t = 0$ of the refined (3+1)-dimensional model

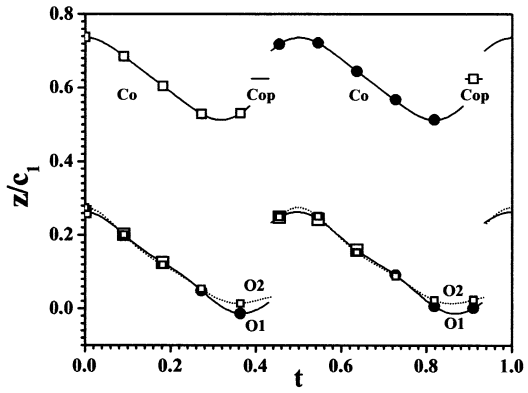

Figure 6. Graphical representation of the fractional z coordinates of the CoO_3 subsystem versus the internal coordinate t ($t = x_4 - q_C \cdot r_{av.}$) in the composite option. Empty squares correspond to the z coordinates of the independent positions (Table 7).

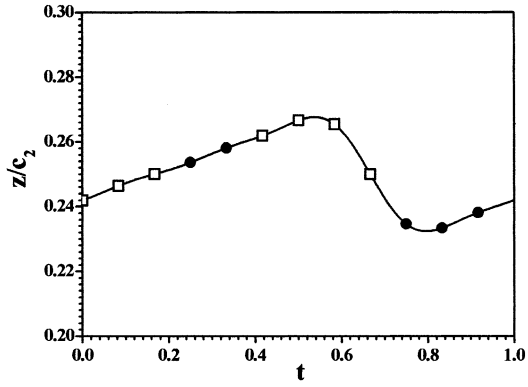

Figure 7. Graphical representation of the fractional z coordinates of the barium atom versus the internal coordinate t in the composite option. Empty squares correspond to the z coordinates of the independent positions (Table 7).

and are represented (for the z coordinates) by the empty squares in Figures 6 and 7. A representation of the structure is shown in Figure 8. As often observed in the structures of the rhombohedral series, the variation of the z component of the CoO_3 subsystem follows a sawtooth function except at the limits of the crenel functions where a significant curvature exists. The variation of the fractional z coordinate of the barium atom (Figure 7) is clearly anharmonic and much smaller than that for the CoO_3 subsystem. For all of the atoms, the modulations of the x and y atomic coordinates are 1 order of magnitude smaller than those along the c axis (see Table 6).

The interatomic distances within the CoO_3 chain are gathered in Table 8. The Co−Co distances within the chains of 10 octahedra sharing faces range between 2.371(3) and 2.52(3) Å. The minimum distance (Co5−Co5′ distance) is in good agreement with the distance of 2.376 Å observed in the 2H-$BaCoO_3$ structure[47] and corresponds to the octahedra in the middle of the columns. From this point, symmetrically, the Co−Co distances increase up to 2.516 Å (Co1−Co2 distance) in the octahedra which are linked with the trigonal prism (Cop). As expected, the Co−Cop distance between the trigonal prism and the adjacent octahedron sharing face

(47) Taguchi, H.; Takeda, Y.; Kanamura, F.; Shimada, M.; Kaizomi, M. *Acta Crystallogr.* **1977**, *B33*, 1299.

Table 6. Average Positions and Components of the Various Amplitude Modulation Functions for $Ba_{12}Co_{11}O_{33}$ in the Composite Option

(a) Average Structure

atom	multiplicity	x_0	y_0	z_0	$U_{eq.}$ (Å^2)	Crenel function $\hat{x}_4$	Crenel function Δ
[CoO_3] Subsystem: $Fddd(00\gamma)0s0$, $\gamma = 6/11$ ($Z = 8$)							
Co	16e	0.87501(9)	7/8	5/8	0.0093(2)	0	5/11
Cop	16f	7/8	0.8753(2)	5/8	0.056(2)	$^1/_4$	1/22
O1	16f	7/8	0.9485(2)	1/8	0.020(1)	$^1/_4$	1/2
O2	32h	0.7650(2)	0.8386(2)	0.1286(9)	0.0186(9)	$^1/_4$	1/2
[Ba] Subsystem: $F'ddd(00\gamma')0s0$, $\gamma' = 11/6$ ($Z = 16$)							
Ba	16f	−1/8	−0.29156(3)	1/4	0.0152(1)		

(b) Components of the Modulation Function Amplitudes

[CoO_3] Subsystem						
Co	$U^{Co}_{x,1} = 0$[a]	$U^{Co}_{y,1} = -0.00005(5)$	$U^{Co}_{z,1} = -0.0815(3)$	$U^{Co}_{x,2} = -0.00002(8)$	$U^{Co}_{y,2} = 0$	$U^{Co}_{z,2} = 0$
	$U^{Co}_{x,3} = 0$	$U^{Co}_{y,3} = 0.00006(4)$	$U^{Co}_{z,3} = -0.0147(4)$	$U^{Co}_{x,4} = -0.00006(13)$	$U^{Co}_{y,4} = 0$	$U^{Co}_{z,4} = 0$
	$U^{Co}_{x,5} = 0$	$U^{Co}_{y,5} = 0.00003(6)$	$U^{Co}_{z,5} = 0.0051(5)$	$U^{Co}_{x,6} = 0.0003(1)$	$U^{Co}_{y,6} = 0$	$U^{Co}_{z,6} = 0$
	$U^{Co}_{u11,1} = 0$	$U^{Co}_{u22,1} = 0$	$U^{Co}_{u33,1} = 0$	$U^{Co}_{u12,1} = -0.0003(3)$	$U^{Co}_{u13,1} = 0.0003(6)$	$U^{Co}_{u23,1} = 0$
	$U^{Co}_{u11,2} = -0.0015(4)$	$U^{Co}_{u22,2} = -0.0032(4)$	$U^{Co}_{u33,2} = -0.0060(4)$	$U^{Co}_{u12,2} = 0$	$U^{Co}_{u13,2} = 0$	$U^{Co}_{u23,2} = -0.0006(4)$
O1	$U^{O1}_{x,1} = 0$	$U^{O1}_{y,1} = 0.0021(2)$	$U^{O1}_{z,1} = 0$	$U^{O1}_{x,2} = -0.0006(5)$	$U^{O1}_{y,2} = 0$	$U^{O1}_{z,2} = 0.099(2)$
	$U^{O1}_{x,3} = 0.0001(6)$	$U^{O1}_{y,3} = 0$	$U^{O1}_{z,3} = 0.007(2)$	$U^{O1}_{x,4} = 0$	$U^{O1}_{y,4} = 0.0005(2)$	$U^{O1}_{z,4} = 0$
	$U^{O1}_{x,5} = -0.0016(7)$	$U^{O1}_{y,5} = 0$	$U^{O1}_{z,5} = 0.009(2)$	$U^{O1}_{x,6} = 0$	$U^{O1}_{y,6} = 0.0006(4)$	$U^{O1}_{z,6} = 0$
	$U^{O1}_{u11,1} = -0.016(2)$	$U^{O1}_{u22,1} = -0.014(2)$	$U^{O1}_{u33,1} = -0.011(3)$	$U^{O1}_{u12,1} = 0$	$U^{O1}_{u13,1} = -0.001(3)$	$U^{O1}_{u23,1} = 0$
	$U^{O1}_{u11,2} = 0$	$U^{O1}_{u22,2} = 0$	$U^{O1}_{u33,2} = 0$	$U^{O1}_{u12,2} = 0.006(3)$	$U^{O1}_{u13,2} = 0$	$U^{O1}_{u23,2} = 0.002(2)$
O2	$U^{O2}_{x,1} = -0.0039(3)$	$U^{O2}_{y,1} = -0.0009(2)$	$U^{O2}_{z,1} = -0.009(1)$	$U^{O2}_{x,2} = -0.0005(3)$	$U^{O2}_{y,2} = 0.0004(2)$	$U^{O2}_{z,2} = 0.093(1)$
	$U^{O2}_{x,3} = -0.0007(4)$	$U^{O2}_{y,3} = -0.0002(3)$	$U^{O2}_{z,3} = 0.007(1)$	$U^{O2}_{x,4} = -0.0017(3)$	$U^{O2}_{y,4} = -0.0008(2)$	$U^{O2}_{z,4} = 0.005(1)$
	$U^{O2}_{x,5} = 0.0006(4)$	$U^{O2}_{y,5} = -0.0002(3)$	$U^{O2}_{z,5} = 0.008(1)$	$U^{O2}_{x,6} = -0.0008(5)$	$U^{O2}_{y,6} = -0.0008(2)$	$U^{O2}_{z,6} = 0.003(2)$
	$U^{O2}_{u11,1} = -0.015(2)$	$U^{O2}_{u22,1} = -0.014(2)$	$U^{O2}_{u33,1} = -0.010(2)$	$U^{O2}_{u12,1} = 0.003(2)$	$U^{O2}_{u13,1} = -0.004(2)$	$U^{O2}_{u23,1} = -0.003(2)$
	$U^{O2}_{u11,2} = -0.001(2)$	$U^{O2}_{u22,2} = 0.001(2)$	$U^{O2}_{u33,2} = 0.004(3)$	$U^{O2}_{u12,2} = 0.003(2)$	$U^{O2}_{u13,2} = -0.002(1)$	$U^{O2}_{u23,2} = -0.001(1)$
[Ba] Subsystem						
Ba	$U^{Ba}_{x,s1} = 0.00840(3)$	$U^{Ba}_{y,s1} = 0.00275(2)$[b]	$U^{Ba}_{z,s1} = -0.01008(5)$	$U^{Ba}_{x,c1} = -U^{Ba}_{x,s1}$	$U^{Ba}_{y,c1} = -U^{Ba}_{y,s1}$	$U^{Ba}_{z,c1} = -U_z$
	$U^{Ba}_{x,s2} = 0$	$U^{Ba}_{y,s2} = -0.00367(2)$	$U^{Ba}_{z,s2} = 0$	$U^{Ba}_{x,c,2} = 0.0022(2)$	$U^{Ba}_{y,c2} = 0$	$U^{Ba}_{z,c2} = 0.00$
	$U^{Ba}_{x,s3} = 0.00103(6)$	$U^{Ba}_{y,s3} = 0.00035(4)$	$U^{Ba}_{z,s3} = 0.0017(1)$	$U^{Ba}_{x,c3} = U^{Ba}_{x,s3}$	$U^{Ba}_{y,c3} = -U^{Ba}_{y,s3}$	$U^{Ba}_{z,c3} = U^{Ba}_{z}$
	$U^{Ba}_{x,s4} = -0.00022(5)$	$U^{Ba}_{y,s4} = 0$	$U^{Ba}_{z,s4} = 0.0009(3)$	$U^{Ba}_{x,c4} = 0$	$U^{Ba}_{y,c4} = -0.00019(7)$	$U^{Ba}_{z,c4} = 0$
	$U^{Ba}_{u11,s1} = 0.0003(3)$	$U^{Ba}_{u22,s1} = -0.0043(2)$	$U^{Ba}_{u33,s1} = -0.0014(1)$	$U^{Ba}_{u12,s1} = 0.0037(2)$	$U^{Ba}_{u13,s1} = 0.0056(1)$	$U^{Ba}_{u23,s1} = -0$
	$U^{Ba}_{u11,c1} = U^{Ba}_{u11,s1}$	$U^{Ba}_{u22,c1} = U^{Ba}_{u22,s1}$	$U^{Ba}_{u33,c1} = U^{Ba}_{u33,s1}$	$U^{Ba}_{u12,c1} = -U^{Ba}_{u12,s1}$	$U^{Ba}_{u13,c1} = U^{Ba}_{u13,s1}$	$U^{Ba}_{u23,c1} = -0$
	$U^{Ba}_{u11,s2} = -0.0023(3)$	$U^{Ba}_{u22,s2} = 0.0010(3)$	$U^{Ba}_{u33,s2} = -0.0016(3)$	$U^{Ba}_{u12,s2} = 0$	$U^{Ba}_{u13,s2} = -0.0010(5)$	$U^{Ba}_{u23,s2} = 0$
	$U^{Ba}_{u11,c2} = 0$	$U^{Ba}_{u22,c2} = 0$	$U^{Ba}_{u33,c2} = 0$	$U^{Ba}_{u12,c2} = 0.0023(5)$	$U^{Ba}_{u13,c2} = 0$	$U^{Ba}_{23,c2} = -0$
	$U^{Ba}_{u11,s3} = 0.0015(4)$	$U^{Ba}_{u22,s3} = 0.0050(4)$	$U^{Ba}_{u33,s3} = -0.0005(3)$	$U^{Ba}_{u12,s3} = -0.0014(3)$	$U^{Ba}_{u13,s3} = -0.0020(3)$	$U^{Ba}_{u23,s3} = -0$
	$U^{Ba}_{u11,c3} = -U^{Ba}_{u11,s3}$	$U^{Ba}_{u22,c3} = -U^{Ba}_{u22,s3}$	$U^{Ba}_{u33,c3} = -U^{Ba}_{u33,s3}$	$U^{Ba}_{u12,c3} = U^{Ba}_{u12,s3}$	$U^{Ba}_{u13,c3} = -U^{Ba}_{u13,s3}$	$U^{Ba}_{23,c3} = U$

(c) Coefficients of the Orthogonalized Functions

Co	$\mathrm{Ortho}^{Co}_0 = 1$
	$\mathrm{Ortho}^{Co}_0 = 1.490 \sin(2\pi x_4)$
	$\mathrm{Ortho}^{Co}_2 = -2.641 + 3.811 \cos(2\pi x_4)$
	$\mathrm{Ortho}^{Co}_3 = -3.303 \sin(2\pi x_4) + 3.288 \sin(4\pi x_4)$
	$\mathrm{Ortho}^{Co}_4 = 4.087 - 5.166 \cos(2\pi x_4) + 2.385 \cos(6\pi x_4)$
	$\mathrm{Ortho}^{Co}_5 = 4.932 \sin(2\pi x_4) - 4.102 \sin(4\pi x_4) + 2.299 \sin(8\pi x_4)$
	$\mathrm{Ortho}^{Co}_6 = -6.044 + 7.648 \cos(2\pi x_4) - 2.424 \cos(6\pi x_4) + 2.154 \cos(10\pi x_4)$
O1	$\mathrm{Ortho}^{O1}_0 = 1$
	$\mathrm{Ortho}^{O1}_1 = -2.069 + 3.249 \sin(2\pi x_4)$
	$\mathrm{Ortho}^{O1}_2 = 1.414 \cos(2\pi x_4)$
	$\mathrm{Ortho}^{O1}_3 = -2.271 \cos(2\pi x_4) + 2.675 \cos(4\pi x_4)$
	$\mathrm{Ortho}^{O1}_4 = -2.187 + 2.785 \sin(2\pi x_4) + 1.953 \sin(6\pi x_4)$
	$\mathrm{Ortho}^{O1}_5 = -2.241 \cos(2\pi x_4) + 1.902 \sin(4\pi x_4) + 1.845 \sin(8\pi x_4)$
	$\mathrm{Ortho}^{O1}_6 = -7.143 + 9.450 \sin(2\pi x_4) + 5.312 \sin(6\pi x_4) + 4.180 \cos(8\pi x_4)$
O2	$\mathrm{Ortho}^{O2}_0 = 1$
	$\mathrm{Ortho}^{O2}_1 = -2.069 + 3.249 \sin(2\pi x_4)$
	$\mathrm{Ortho}^{O2}_2 = 1.414 \cos(2\pi x_4)$
	$\mathrm{Ortho}^{O2}_3 = -2.271 \cos(2\pi x_4) + 2.675 \cos(4\pi x_4)$
	$\mathrm{Ortho}^{O2}_4 = -2.187 + 2.785 \sin(2\pi x_4) + 1.953 \sin(6\pi x_4)$
	$\mathrm{Ortho}^{O2}_5 = -2.241 \cos(2\pi x_4) + 1.902 \sin(4\pi x_4) + 1.845 \sin(8\pi x_4)$
	$\mathrm{Ortho}^{O2}_6 = -7.143 + 9.450 \sin(2\pi x_4) + 5.312 \sin(6\pi x_4) + 4.180 \cos(8\pi x_4)$

[a] Modulation function for a parameter λ of an atom ν defined in a restricted interval are given by the following: $U^{\nu}_{\lambda}(x_4) = \sum_{n=0}^{k} U^{\nu}_{\lambda,n}$ Ortho$^{\nu}_n(x_4)$ where the orthogonalized functions, obtained through a Schmidt orthogonalization routine, are given by the following: Ortho$^{\nu}_i(x_4) = B^{\nu}_0 + \sum_{n=1}^{k} A^{\nu}_n \sin(2\pi n x_4) + \sum_{n=1}^{k} B^{\nu}_n \cos(2\pi n x_4)$ with coefficients B^{ν}_0, A^{ν}_n, and B^{ν}_n given below. [b] For Ba, the modulation functions are interpreted by the Fourier series: $U^{\nu}_{\lambda}(x_4) = U,^{\nu}_{\lambda 0} + \sum_{n=1}^{k} U^{\nu}_{\lambda,sn} \sin(2\pi n x_4) + \sum_{n=1}^{k} U^{\nu}_{\lambda,cn} \cos(2\pi n x_4)$.

Table 7. Atomic Fractional Positions Corresponding to the 3-Dimensional Structure of $Ba_{12}Co_{11}O_{33}$ Yielded by the Two Alternative Refinements Performed within the Superspace Formalism[a]

atom	*x*	*y*	*z*	atom	*x*	*y*	*z*
Co1	0.8751	0.8750	0.9744	O3	7/8	0.9511	3/8
	0.8752	*0.8749*	*0.9740*		*7/8*	*0.9517*	*3/8*
Co2	0.8752	0.8750	0.6830	O4	0.7661	0.8381	0.0248
	0.8771	*0.8750*	*0.6837*		*0.7666*	*0.8359*	*0.0238*
Co3	0.8747	0.8749	0.1565	O5	0.7610	0.8387	0.1999
	0.8767	*0.8749*	*0.1570*		*0.7615*	*0.8393*	*0.1994*
Co4	0.8747	0.8751	0.5059	O6	0.7615	0.8378	0.3743
	0.8749	*0.8752*	*0.5060*		*0.7607*	*0.8359*	*0.3745*
Co5	0.8753	0.8749	0.3314	O7	0.7645	0.8384	0.5502
	0.8736	*0.8749*	*0.3309*		*0.7640*	*0.8384*	*0.5512*
Cop	7/8	0.8753	7/8	O8	0.7649	0.8373	0.7285
	7/8	*0.8752*	*7/8*		*0.7649*	*0.8382*	*0.7283*
Ba1	0.8874	0.7087	0.0403	O9	0.1251	0.1946	0.0683
	0.8885	*0.7087*	*0.0404*		*0.1275*	*0.1949*	*0.0681*
Ba2	0.8832	0.7116	0.2056	O10	0.1267	0.1989	0.3630
	0.8821	*0.7116*	*0.2055*		*0.1297*	*0.1987*	*0.3631*
Ba3	7/8	0.7093	3/8	O11	0.1231	0.2005	0.5372
	7/8	*0.7093*	*3/8*		*0.1202*	*0.2000*	*0.5383*
Ba4	7/8	0.7006	7/8	O12	0.2282	0.0895	0.0702
	7/8	*0.7006*	*7/8*		*0.2305*	*0.0904*	*0.0694*
Ba5	0.1312	0.9531	0.0423	O13	0.2258	0.0926	0.1817
	0.1322	*0.9531*	*0.0424*		*0.2258*	*0.0919*	*0.1815*
Ba6	0.1117	0.9623	0.3730	O14	0.2374	0.0879	0.3636
	0.1115	*0.9622*	*0.3730*		*0.2394*	*0.0868*	*0.3645*
Ba7	0.1223	0.9599	0.5391	O15	0.2394	0.0885	0.5365
	0.1236	*0.9599*	*0.5391*		*0.2349*	*0.0890*	*0.5370*
O1	0.8722	0.9482	0.0239	O16	0.2366	0.0879	0.7124
	0.8753	*0.9480*	*0.0229*		*0.2391*	*0.0890*	*0.7120*
O2	0.8761	0.9494	0.2001	O17	0.2361	0.0879	0.8884
	0.8740	*0.9500*	*0.1994*		*0.2339*	*0.0872*	*0.8872*

[a] Positions in italics correspond to the *layer option* refinement.

is noticeably longer (2.70(3) Å). On the other hand, the minimum Ba−O distance is 2.59(2) Å.

A bond valence calculation has been carried out using the formalism of Brese and O'Keefe[48] and the distances given in Table 8. The bond valence for the cobalt occupying the trigonal prism (Cop) is 2.35, which can be associated with the valence state +2. Equivalent calculations for the octahedral cobalt atoms lead to bond valences ranging between 4.02 (Co1) and 3.63 (Co5), which is in good agreement with Co^{IV}. The bond-valence parameter for Co^{IV} bonds to oxygen has been estimated to be $R_{ij} = 1.724$ from the 2H-$BaCoO_3$ structure.[47] These results agree with previous results where it was predicted[4] and confirmed experimentally that the trigonal prisms are occupied by divalent cations and the octahedra by tetravalent cations.[10,49,50]

4.2. Layer Model. The structure is considered to be a modulated structure with an average orthorhombic unit cell (parameters $a = 11.4129(2)$ Å, $b = a\sqrt{3} = 19.7677(2)$ Å, $c_L = 4.5324(1)$ Å) and a modulation wavevector $q_L = (1/6)c_L^*$ with the superspace group symmetry $Xdcd(00\gamma_L)qq0$, as given in Table 2. Each Bragg reflection H can then be indexed as $H = ha^* + kb^* + lc_L^* + mq_L$. The measured ($h$ k l) reflections

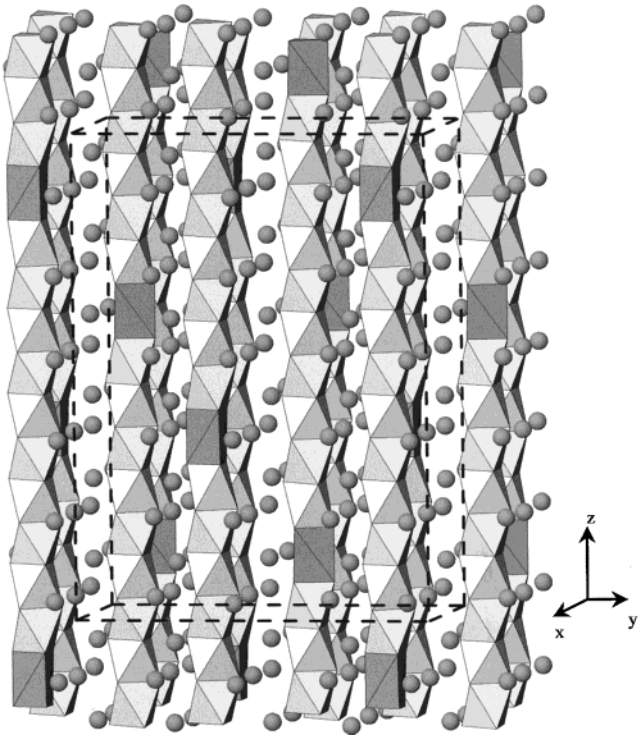

Figure 8. Representation of the structure of $Ba_{12}Co_{11}O_{33}$.

referring to the orthorhombic supercell were transformed into (h k l m) indices using the JANA 2000 program package.[46] This transformation leads to 4625 independent observed reflections for $I \geq 3\sigma(I)$. The classification of the reflections as main reflections and satellites of different orders obviously changes with respect to that considered for the composite description (see Table 5). In this description, the number of satellites significantly increases at the cost of the main reflections. The number of satellites of third order are nearly doubled. This may suggest that the system deviates more strongly from the idealized layer model without displacive modulations than from the composite one. However, this cannot be taken too literally, as both alternative models, the ideal layer model and the composite without displacive modulations, are both strongly modulated structures. Both contain by definition occupational discrete atomic domains (the crenel functions), and this is already sufficient to explain nonzero satellite intensities in all orders. In any case, the refinement of the displacive part of the modulation starting from the reference ideal layer model could be performed and converged without additional difficulties.

In line with the results obtained for the composite model, a sawtooth function for the displacive modulation of the cobalt occupying the octahedral site was considered. This function is centered at $x_4 = 3/8$ with a width

Table 8. Interatomic Distances (Å) and Bond-Valence Values within the [CoO_3] Chain

Cop−Co1	2.704	Co1−Co2	2.517	Co2−Co3	2.434	Co3−Co4	2.383	Co4−Co5	2.372	Co5−Co5′	2.374
Co1−O1	1.976	Co2−O1	1.862	Co3−O2	1.891	Co4−O2	1.894	Co5−O3	1.918	Cop−O9	2.071
Co1−O4	1.991	Co2−O4	1.839	Co3−O5	1.894	Co4−O5	1.914	Co5−O6	1.896	Cop−O9′	2.071
Co1−O8	1.942	Co2−O8	1.917	Co3−O7	1.874	Co4−O7	1.887	Co5−O6′	1.913	Cop−O12	2.021
Co1−O9	1.802	Co2−O10	1.925	Co3−O10	1.878	Co4−O11	1.900	Co5−O11	1.915	Cop−O12′	2.021
Co1−O12	1.833	Co2−O14	1.948	Co3−O14	1.886	Co4−O15	1.883	Co5−O15	1.925	Cop−O13	2.025
Co1−O13	1.756	Co2−O17	1.900	Co3−O17	1.905	Co4−O16	1.886	Co5−O16	1.894	Cop−O13′	2.025
Co1−Oav.	1.883	Co2−Oav.	1.900	Co3−Oav.	1.888	Co4−Oav.	1.894	Co5−Oav.	1.910	Cop−Oav.	2.039
$\sum v_{ij}$ Co1	4.02	$\sum v_{ij}$ Co2	3.77	$\sum v_{ij}$ Co3	3.85	$\sum v_{ij}$ Co4	3.79	$\sum v_{ij}$ Co5	3.63	$\sum v_{ij}$ Cop	2.35

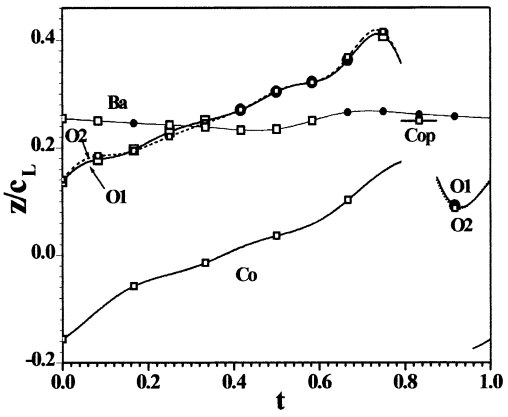

Figure 9. Graphical representation of the fractional *z* coordinates of the CoO_3 chain versus the internal coordinate *t* ($t = x_4 - q_L \cdot r_{av.}$) in the layer option. Empty symbols correspond to the *z* coordinates of the independent positions (Table 7).

of $\Delta = 5/6$ ($\Delta = (1 - x)/(1 + x)$ with $x = 1/11$). Except for this special feature, all other atomic displacive modulations, including the deviation of octahedral Co from the sawtooth linear behavior, were parametrized throughout the refinement with conventional symmetry-constrained Fourier series. In this case, the large width of the occupational functions makes the use of orthogonalized functions within the crenel interval instead of the sine and cosine functions unnecessary. Modulations in the plane *xy* allowed by symmetry were initially kept to zero. The occupation domains of the cobalt within the trigonal prisms and the oxygen atoms were described by the crenel functions suggested by the model discussed above (see Table 4). The refinement was carried out considering the commensurate case and the section at $t = 0$. In the previous steps of the refinement, only the maximum amplitude of the sawtooth displacive modulation of the octahedral cobalt and the first harmonic of the modulation of the barium atom were considered as refinable parameters. The residual factor *R* stabilized around 15%. Then after successive steps, the displacive Fourier amplitude waves for all of the atoms were introduced in the refinement up to fourth order for the octahedral cobalt and the barium atom and fifth order for the oxygen atoms. The *R* value decreased to $R \approx 7\%$. In a final step, Fourier amplitudes for the atomic displacement parameters for the cobalt, oxygen, and barium atoms were included in the refinement. Then the final residual factor *R* was stabilized at 4.53% for 149 independent refined parameters. The corresponding atomic positions of the 3-dimensional superstructure resulting from the section at $t = 0$ are given in Table 7 (italic figures) and compared to those of the composite model. The results are very similar and confirm the validity of the two structural approaches. Figure 9 depicts the resulting displacive modulations of the atoms with respect to their ideal layer position. The commensurate case ($t = 0$) is marked by symbols; the empty ones correspond to the independent atomic positions (*z* coordinate) given in Table 7. Ba sites are very weakly modulated relative to the rest, keeping approximately the reference ideal height of the layer, which is also kept by the Co in the prism, as expected from the layer description. On the other hand, both the octahedral Co and the oxygens follow approximately a strong sawtooth-like modulation, maintaining an approximately constant distance along *z* between the oxygens and Co. This strong sawtooth modulation is the signature of the composite character of the structure in the layer description. It clearly shows that the chains of oxygens plus octahedral Co are quite rigid and strongly deviate from their ideal position in the layer description. The approximate amplitudes of these atomic modulations are larger than those obtained in the composite description (Figure 6), by approximately a factor 2. Nevertheless, the use a priori in the refinement of mathematical sawtooth functions can overcome the eventual difficulty of larger modulations and allows a change from one type of description to the other while maintaining similar performances in the refinements.

It is remarkable that the longitudinal modulation functions of O_1 and O_2, although symmetry independent, nearly superpose. This is the signature of the strong planar rigidity of the O_3 triangles that form the faces of both the octahedra and prisms in the [CoO_3] chains, displacing essentially as a whole along the *z* direction.

As observed in the composite model (see Table 6), the value of the U_{eq} of the cobalt occupying the trigonal prism (Cop) is relatively high (0.063(2) Å^2) with a strong delocalization along the *z* direction ($U_{33} = 0.168(5)$ Å^2). To explain these values, the prismatic cobalt position was introduced as a general position with an occupancy of 1/2. The residual factor set at 4.36% (Table 3) and the atomic displacement parameter U_{eq} of Cop stabilized at a reasonable value of 0.014 Å^2 comparable to those of the other atoms (Table 9). Such splitting of the trigonal prismatic position has been observed in similar structures belonging to the rhombohedral series.[14] Obviously, the Co−Co distance between the prismatic cobalt and the adjacent octahedral cobalt sharing a face is reduced to 2.365 Å, which is comparable to the observed Co−Co distance between octahedra sharing faces (Table 8). The average positions and the components of the atomic modulation amplitudes are gathered in Table 9.

5. Conclusions

The crystal structure determination of $Ba_{12}Co_{11}O_{33}$ shows clearly that the sequence of layers along the *c* axis is of the general type $\langle 21 \rangle_L$ with a resulting stacking period of 12 layers yielding (CoO_3) chains with the sequence 10Oh−1Tp. The structure corresponds to the member $m = 2$ and $n = 1$ of the general formula $A_{4m+4n}A'_nB_{4m+2n}O_{12m+9n}$ where m/n is the proportion of A_8O_{24} to $A_8A'_2O_{18}$ layers. As in the rhombohedral series, the uniform layer sequence can be derived using the Farey tree scheme. This new family can be associated to a polytypism of the $A_{1+x}(A'_xB_{1-x})O_3$ series, as is well-known for other ABO_3 hexagonal perovskites. This study has shown that these long period structures can be quantitatively described and determined combining superspace formalism and an idealized layered structure as basic reference. This approach yields equivalent results to the usual composite description. The description as a layered structure also allows a direct derivation of the possible maximal superspace group symmetry of

(48) Brese, N. E.; O'Keefe, M. *Acta Crystallogr.* **1991**, *B47*, 192.
(49) El Abed, A.; Gaudin, E.; Lemaux, S.; Darriet, J. *Solid State Sci.* **2001**, *3*, 887.
(50) El Abed, A.; Gaudin, E.; Darriet, J.; Whangbo, M.-H., *J. Solid State Chem.* **2002**, *163*, 513.

Table 9. Average Positions and Components of the Various Amplitude Modulation Functions for $Ba_{12}Co_{11}O_{33}$ in the Layer Option[a]

(a) Average Structure

atom	x_0	y_0	z_0	$U_{eq.}$(Å^2)	Crenel function $\hat{x}_4$	Crenel function Δ	amplitude
Co	0.8751(2)	7/8	0	0.0125(6)	3/8	5/6	0.155
Cop	0.876(1)	0.8752(3)	0.322(1)	0.014(2)	7/8	1/12	
O1	7/8	−0.0521(7)	1/4	0.021(2)	3/8	11/12	
O2	0.7661(8)	0.8390(4)	0.252(1)	0.019(1)	3/8	11/12	
Ba	7/8	0.70841(5)	1/4	0.0151(2)			

(b) Components of the Modulation Function Amplitudes

Co	$U^{Co}_{x,s1}$= 0.0001(3)	$U^{Co}_{y,s1}$= −0.00007(8)	$U^{Co}_{z,s1}$= −0.0042(2)	$U^{Co}_{x,c1}$= $-U^{Co}_{x,s1}$	$U^{Co}_{y,c1}$= $U^{Co}_{y,s1}$	$U^{Co}_{z,c1}$= $U^{Co}_{z,s1}$
	$U^{Co}_{x,s2}$= 0.0022(5)	$U^{Co}_{y,s2}$= 0	$U^{Co}_{z,s2}$= 0	$U^{Co}_{x,c2}$= 0	$U^{Co}_{y,c2}$= 0.00005(9)	$U^{Co}_{z,c2}$= −0.0136(4)
	$U^{Co}_{x,s3}$= 0.0002(2)	$U^{Co}_{y,s3}$= 0.00005(12)	$U^{Co}_{z,s3}$= 0.0072(5)	$U^{Co}_{x,c3}$= $U^{Co}_{x,s3}$	$U^{Co}_{y,c3}$= $-U^{Co}_{y,s3}$	$U^{Co}_{z,c3}$= $-U^{Co}_{z,s3}$
	$U^{Co}_{u11,s1}$= −0.003(1)	$U^{Co}_{u22,s1}$= −0.005(1)	$U^{Co}_{u33,s1}$= −0.013(1)	$U^{Co}_{u12,s1}$= 0.0005(5)	$U^{Co}_{u13,s1}$= 0.0014(9)	$U^{Co}_{u23,s1}$= 0.001(1)
	$U^{Co}_{u11,c1}$= $-U^{Co}_{u11,s1}$	$U^{Co}_{u22,c1}$= $-U^{Co}_{u22,s1}$	$U^{Co}_{u33,c1}$= $-U^{Co}_{u33,s1}$	$U^{Co}_{u12,c1}$= $U^{Co}_{u12,s1}$	$U^{Co}_{u13,c1}$= $U^{Co}_{u13,s1}$	$U^{Co}_{u23,c1}$= $-U^{Co}_{u23,s1}$
	$U^{Co}_{u11,s2}$= −0.004(2)	$U^{Co}_{u22,s2}$= −0.003(2)	$U^{Co}_{u33,s2}$= −0.008(2)	$U^{Co}_{u12,s2}$= 0	$U^{Co}_{u13,s2}$= 0	$U^{Co}_{u23,s2}$= 0.001(2)
	$U^{Co}_{u11,c2}$= 0	$U^{Co}_{u22,c2}$= 0	$U^{Co}_{u33,c2}$= 0	$U^{Co}_{u12,c2}$= 0.004(1)	$U^{Co}_{u13,c2}$= −0.007(1)	$U^{Co}_{u23,c2}$= 0
O1	$U^{O1}_{x,s1}$= −0.004(7)	$U^{O1}_{y,s1}$= 0.0027(7)	$U^{O1}_{z,s1}$= −0.072(1)	$U^{O1}_{x,c1}$= $U^{O1}_{x,s1}$	$U^{O1}_{y,c1}$= $-U^{O1}_{y,s1}$	$U^{O1}_{z,c1}$= $U^{O1}_{z,s1}$
	$U^{O1}_{x,s2}$= 0	$U^{O1}_{y,s2}$= 0.0016(10)	$U^{O1}_{z,s2}$= 0	$U^{O1}_{x,c2}$= −0.0003(15)	$U^{O1}_{y,c2}$= 0	$U^{O1}_{z,c2}$= −0.057(2)
	$U^{O1}_{x,s3}$= −0.003(1)	$U^{O1}_{y,s3}$= 0.0010(8)	$U^{O1}_{z,s3}$= 0.025(2)	$U^{O1}_{x,c3}$= $-U^{O1}_{x,s3}$	$U^{O1}_{y,c3}$= $U^{O1}_{y,s3}$	$U^{O1}_{z,c3}$= $-U^{O1}_{z,s3}$
	$U^{O1}_{x,s4}$= 0.0011(7)	$U^{O1}_{y,s4}$= 0	$U^{O1}_{z,s4}$= 0.023(2)	$U^{O1}_{x,c4}$= 0	$U^{O1}_{y,c4}$= 0.0007(13)	$U^{O1}_{z,c4}$= 0
	$U^{O1}_{x,s5}$= 0.0001(5)	$U^{O1}_{y,s5}$= −0.0007(7)	$U^{O1}_{z,s5}$= 0.004(2)	$U^{O1}_{x,c5}$= $U^{O1}_{x,s5}$	$U^{O1}_{y,c5}$= $-U^{O1}_{y,s5}$	$U^{O1}_{z,c5}$= $U^{O1}_{z,s5}$
	$U^{O1}_{u11,s1}$= −0.015(4)	$U^{O1}_{u22,s1}$= −0.014(4)	$U^{O1}_{u33,s1}$= −0.007(4)	$U^{O1}_{u12,s1}$= 0.008(4)	$U^{O1}_{u13,s1}$= −0.003(6)	$U^{O1}_{u23,s1}$= 0.002(2)
	$U^{O1}_{u11,c1}$= $-U^{O1}_{u11,s1}$	$U^{O1}_{u22,c1}$= $-U^{O1}_{u22,s1}$	$U^{O1}_{u33,c1}$= $-U^{O1}_{u33,s1}$	$U^{O1}_{u12,c1}$= $U^{O1}_{u12,s1}$	$U^{O1}_{u13,c1}$= $-U^{O1}_{u13,s1}$	$U^{O1}_{u23,c1}$= $U^{O1}_{u23,s1}$
O2	$U^{O2}_{y,s1}$= −0.004(1)	$U^{O2}_{y,s1}$= −0.0014(5)	$U^{O2}_{z,s1}$= −0.075(2)	$U^{O2}_{x,c1}$= 0.004(1)	$U^{O2}_{y,c1}$= 0.0015(5)	$U^{O2}_{z,c1}$= −0.071(2)
	$U^{O2}_{x,s2}$= −0.003(1)	$U^{O2}_{y,s2}$= −0.0018(6)	$U^{O2}_{z,s2}$= 0.004(2)	$U^{O2}_{x,c2}$= 0.0007(10)	$U^{O2}_{y,c2}$= −0.0001(8)	$U^{O2}_{z,c2}$= −0.057(1)
	$U^{O2}_{x,s3}$= −0.003(1)	$U^{O2}_{y,s3}$= −0.0016(6)	$U^{O2}_{z,s3}$= 0.029(2)	$U^{O2}_{x,c3}$= 0.0003(12)	$U^{O2}_{y,c3}$= −0.0012(6)	$U^{O2}_{z,c3}$= −0.027(2)
	$U^{O2}_{x,s4}$= 0.0005(5)	$U^{O2}_{y,s4}$= −0.0005(3)	$U^{O2}_{z,s4}$= 0.023(2)	$U^{O2}_{x,c4}$= −0.0005(17)	$U^{O2}_{y,c4}$= 0.0003(8)	$U^{O2}_{z,c4}$= 0.0003(22)
	$U^{O2}_{x,s5}$= 0.0007(9)	$U^{O2}_{y,s5}$= 0.0005(4)	$U^{O2}_{z,s5}$= 0.003(2)	$U^{O2}_{x,c5}$= −0.0006(9)	$U^{O2}_{y,c5}$= −0.0006(5)	$U^{O2}_{z,c5}$= 0.004(2)
	$U^{O2}_{u11,s1}$= −0.013(4)	$U^{O2}_{u22,s1}$= −0.013(4)	$U^{O2}_{u33,s1}$= −0.012(5)	$U^{O2}_{u12,s1}$= 0.004(3)	$U^{O2}_{u13,s1}$= −0.001(4)	$U^{O2}_{u23,s1}$= −0.002(5)
	$U^{O2}_{u11,c1}$= 0.015(4)	$U^{O2}_{u22,c1}$= 0.013(4)	$U^{O2}_{u33,c1}$= 0.008(4)	$U^{O2}_{u12,c1}$= −0.002(3)	$U^{O2}_{u13,c1}$= −0.001(4)	$U^{O2}_{u23,c1}$= 0.002(5)
Ba	$U^{Ba}_{x,s1}$= 0.00839(5)	$U^{Ba}_{y,s1}$= 0.00276(4)	$U^{Ba}_{z,s1}$= −0.01021(9)	$U^{Ba}_{x,c1}$= 0.00839(5)	$U^{Ba}_{y,c1}$= −0.00276(4)	$U^{Ba}_{z,c1}$= 0.01021(9)
	$U^{Ba}_{x,s2}$= 0	$U^{Ba}_{y,s2}$= 0.00364(4)	$U^{Ba}_{z,s2}$= 0	$U^{Ba}_{x,c,2}$= 0.0035(2)	$U^{Ba}_{y,c2}$= 0	$U^{Ba}_{z,c2}$= 0.0060(2)
	$U^{Ba}_{x,s3}$= 0.0012(1)	$U^{Ba}_{y,s3}$= 0.00034(5)	$U^{Ba}_{z,s3}$= 0.0019(2)	$U^{Ba}_{x,c3}$= $-U^{Ba}_{x,s3}$	$U^{Ba}_{y,c3}$= $U^{Ba}_{y,s3}$	$U^{Ba}_{z,c3}$= $-U^{Ba}_{z,s3}$
	$U^{Ba}_{x,s4}$= −0.00018(9)	$U^{Ba}_{y,s4}$= 0	$U^{Ba}_{z,s4}$= −0.0006(6)	$U^{Ba}_{x,c4}$= 0	$U^{Ba}_{y,c4}$= −0.0002(2)	$U^{Ba}_{z,c4}$= 0
	$U^{Ba}_{u11,s1}$= 0.0016(4)	$U^{Ba}_{u22,s1}$= −0.0043(3)	$U^{Ba}_{u33,s1}$= −0.0014(2)	$U^{Ba}_{u12,s1}$= 0.0041(3)	$U^{Ba}_{u13,s1}$= 0.0053(2)	$U^{Ba}_{u23,s1}$= −0.0037(3)
	$U^{Ba}_{u11,c1}$= $-U^{Ba}_{u11,s1}$	$U^{Ba}_{u22,c1}$= $-U^{Ba}_{u22,s1}$	$U^{Ba}_{u33,c1}$= $-U^{Ba}_{u33,s1}$	$U^{Ba}_{u12,c1}$= $U^{Ba}_{u12,s1}$	$U^{Ba}_{u13,c1}$= $-U^{Ba}_{u13,s1}$	$U^{Ba}_{u23,c1}$= $U^{Ba}_{u23,s1}$
	$U^{Ba}_{u11,s2}$= 0.0018(5)	$U^{Ba}_{u22,s2}$= −0.0011(5)	$U^{Ba}_{u33,s2}$= 0.0017(4)	$U^{Ba}_{u12,s2}$= 0	$U^{Ba}_{u13,s2}$= −0.0013(7)	$U^{Ba}_{u23,s2}$= 0
	$U^{Ba}_{u11,c2}$= 0	$U^{Ba}_{u22,c2}$= 0	$U^{Ba}_{u33,c2}$= 0	$U^{Ba}_{u12,c2}$= −0.0002(7)	$U^{Ba}_{u13,c2}$= 0	$U^{Ba}_{23,c2}$= −0.0088(3)
	$U^{Ba}_{u11,s3}$= 0.0006(5)	$U^{Ba}_{u22,s3}$= 0.0053(6)	$U^{Ba}_{u33,s3}$= −0.0003(3)	$U^{Ba}_{u12,s3}$= −0.0024(6)	$U^{Ba}_{u13,s3}$= −0.0020(3)	$U^{Ba}_{u23,s3}$= 0.0020(5)
	$U^{Ba}_{u11,c3}$= $U^{Ba}_{u11,s3}$	$U^{Ba}_{u22,c3}$= $U^{Ba}_{u22,s3}$	$U^{Ba}_{u33,c3}$= $U^{Ba}_{u33,s3}$	$U^{Ba}_{u12,c3}$= $-U^{Ba}_{u12,s3}$	$U^{Ba}_{u13,c3}$= $U^{Ba}_{u13,s3}$	$U^{Ba}_{23,c3}$= $-U^{Ba}_{u23,s3}$

[a] The modulation functions are interpreted by the Fourier series: $U^{\nu}_{\lambda}(x_4) = U^{\nu}_{,\lambda 0} + \sum_{n=1}^{k} U^{\nu}_{,\lambda sn} \sin(2\pi n x_4) + \sum_{n=1}^{k} U^{\nu}_{,\lambda cn} \cos(2\pi n x_4)$.

the compound series, from the symmetry of the layers involved. By this means we have successfully postulated the superspace group associated with this orthorhombic family.

The present study demonstrates that the idealized layered model inferred for $Ba_{12}O_{11}O_{33}$ from high-resolution electron microscopy images[32] was not correct. This also casts serious doubts upon the models proposed in the same work for other more complex systems such as $Ba_9Co_8O_{24}$ and $Ba_{11}Co_{10}O_{33}$, also at variance with the general rules observed in the trigonal series, and where even the distribution of trigonal prisms along the [A′B]-O_3 chains would not be uniform.

Acknowledgment. This work has been supported by the DGESIC (Project PB98-0244) and the UPV (Project 9/UPV 00063.310-13564/2001). We gratefully thank Vaclav Petricek for valuable comments and help using JANA.

Supporting Information Available: X-ray crystallographic data (PDF). This material is available free of charge via the Internet at http://pubs.acs.org.

CM0211610